A ubiquitin pathway associated with genome integrity in fission yeast

Park Joon-Hyun

DOCTOR OF PHILOSOPHY

Department of Genetics

School of Life Science

The Graduate University for Advanced Studies

2003

CONTENTS

ABSTRACT

Homologous recombination must be strictly regulated in order to maintain chromosome integrity otherwise can lead to metabolic burden and subsequent cell death. However, the molecular mechanism(s) of this regulation in mitosis is yet unclear although it is an essential event during meiotic process. In this study, I present several lines of evidence that Ubc7, one of the 14 ubiquitin-conjugating enzymes in the fission yeast *S.pombe*, is implicated in the negative regulation of homologous recombination. Mitotic recombination caused by Ubc7-defect was enhanced between tandem-repeat segments at the *mat1* and *ade6* loci, depending upon *smt*-associated imprint and Rad2-deficiency, respectively, both of which induce competence for the initiation of recombination. Moreover, Ubc7 mutant cells exhibited hyper-resistance to UV irradiation and MMS-induced DNA damage. The increased repair activity was also dependent on the function of Rhp51, a eukaryotic RecA counterpart that plays a key role in homologous recombination and recombinational repair. These results suggest that mitotic homologous recombination is a two-step reaction in eukaryotes: the initiation step establishes competence for homologous recombination and DNA exchange, while the second step mediates the recombination itself. This study demonstrates a first direct evidence that Ubc7-mediated ubiquitylation negatively regulates mitotic recombination in the middle-stage process related to DNA strand exchange, but not in the preceding initiation reaction in the fission yeast.

ABBREVIATIONS

E.coli ; *Escherichia coli*

S.cerevisiae ; *Saccharomyces cerevisiae*

S.pombe ; *Schizosaccharomyces pombe*

H.sapiens ; *Homo sapiens*

ARS ; autonomously replicating sequence

bp ; base pair

DAPI ; 4',6-diamino-2-phenylindole

DSB ; double-strand break

E1 ; ubiquitin-activating enzyme

E2(Ubc) ; ubiquitin-conjugating enzyme

E3 ; ubiquitin ligase

5-FOA ; 5-fluoroorotic acid

HECT ; homologous to E6-AP carboxy terminus

HR ; homologous recombination

kb ; kilobase

MMS ; methylmethane sulfonate

MT ; mating-type

NHEJ ; nonhomologous end joining

nmt ; thiamine-repressible promoter

ORF ; open reading frame

PCNA ; proliferating cell nuclear antigen

PCR ; polymerase chain reaction

PFGE ; Pulse-field gel electrophoresis

rDNA ; ribosomal DNA

SDS ; sodium dodecyl sulfate

SDS-PAGE ; SDS polyacrylamide gel electrophoresis

smt ; swiching for mating-type

SUMO ; small ubiquitin-like modifier

UV ; ultraviolet ray

INTRODUCTION

The genomic DNA is highly susceptible to spontaneous and environmental stresses in living cells. If not properly repaired, DNA damages may result in chromosomal aberrations, which, in turn, can lead to cell death or uncontrolled cell growth (Friedberg et al., 1995). To maintain the integrity of the genome, multiple pathways have evolved for the repair of damaged DNA, including DNA repair, checkpoints, and tolerance pathways that allow cells to survive DNA damage. Homologous recombination is one of the major pathways for this survival program. During meiosis, which is a special type of cell division that produces haploid gametes from diploid parental cells, homologous recombination occurs at a high frequency and can generate new allelic combinations in the resulting gametes, thereby increasing the genetic diversity of the progeny and promoting the survival of the species during critical environmental changes (Nasim et al., 1989). Homologous recombination is also essential for ensuring correct chromosome segregation during meiosis. Recombination does not take place evenly throughout the genome of many organisms, but at higher than average frequencies in some regions and lower in others. Unlike the meiotic process, however, mitotic recombination is ordinarily suppressed by an as yet unidentified mechanism(s). Much headway has been progressed for identifying and clarifying the biological function of homologous recombination during the past decades. Since a vast range of information has been accumulated on this, it

is not fully understood how homologous recombination is regulated during mitosis.

To avoid double-strand breaks (DSBs), eukaryotic cells have evolved two major pathways (Kanaar and Hoeijmakers, 1997; Kanaar et al., 1998): nonhomologous end-joining (NHEJ) and homologous recombination (HR). NHEJ joins adjacent broken DNA ends, resulting errors in the junction region although it is important for cell survival. In contrast, conservative HR pathway uses the undamaged homologous DNA strand as a template to repair the damaged copy of DNA, resulting in accurate repair of DSBs. Therefore, proper HR activity is essential for reducing DNA damage-induced mutagenesis for maintaining chromosome stability. In lower eukaryotes, HR is the major pathway for repairing DSBs and NHEJ is involved in the repair of DSBs introduced by ionizing radiation only when defective in HR. However, in higher eukaryotes such as mammals, NHEJ play major roles in repairing DSBs. The HR pathways have been studied extensively in the budding yeast *S.cerevisiae* (Paques and Haber, 1999). This machinery designated as the *RAD52* pathway includes *RAD51, RAD52, RAD54, RAD55, RAD57, MRE11* and *Xrs2*, which are well conserved throughout eukayotes. Mutations in these genes increase sensitivity to ionizing radiation and cause defects in recombination. A key player of the eukaryotic HR machinery is the RAD51 protein. RAD51 is the structural and functional eukaryotic counterpart of *E.coli* RecA (Shinohara et

al., 1992). *In vitro* studies with yeast and human RAD51 indicate that, as with RecA, RAD51 promotes homologous DNA pairing and strand exchange. RAD52 is thought to mediate RAD51 function (Paques and Haber, 1999). In the fission yeast *S.pombe*, all the counterpart genes are known to be present but their functions are not fully understood. Deletion of a RAD51 homologue, *rhp51*$^{+}$, in the fission yeast induced delayed growth, heterogeneity in cell size and aberrant nuclear phenotypes, suggesting that *S.pombe* RAD51 may be involved in segregation of chromosomes or maintenance of genome integrity. Similarly, disruption of mammalian RAD51 causes severe chromosomal abnormalities and early embryonic death. On the other hand, it has been previously reported that the recombination protein Rad51 and Rad22 (*S.pombe* homologue of the RAD52) could be modified by a SUMO (Ho et al., 2001; Kovalenko et al., 1996).

The ubiquitin-mediated proteolysis is a key mechanism by which the level of target proteins is regulated in a temporary manner. Numerous studies have uncovered that ubiquitylation plays major roles in a broad array of basic cellular events, including cell-cycle control, signal transduction, DNA repair, transcriptional regulation, nuclear transport process, endocytosis, and immune responses (Hershko and Ciechanover, 1998; Hochstrasser, 1996; Pickart, 2001). In one sense, ubiquitylation might be as important as protein phosporylation, which controls the activities of thousands of proteins. The classical view of ubquitylation is that it targets proteins for degradation by a multi-subunit

proteosome. Ubiquitin, a 76-amino-acid globular protein, is highly conserved in eukarotes, with only three amino acid changes from yeast to human. Ubiquitin is transferred to substrate proteins in a polyubquitinated form through three sequential enzymatic steps; 1) ATP-dependent activation of ubiquitin through the formation of a thiol ester with ubiquitin-activating enzyme or E1; 2) ubquitin transfer to a cysteine residue of a ubiquitin-conjugating enzyme or E2; 3) ubiquitin transfer from E2 to the target substrate catalyzed by a ubiquitin ligase or E3. Finally, polyubiquitinated substrates are degraded to short peptides by the 26S proteasome complex, and the free ubiquitin is recycled for further ubiquitylation (Fig. 1). There is also emerging evidence that ubiquin-modification regulates process other than protein degradation (Hoege et al., 2002).

Specific E2s and E3s cooperate in the recognition of individual substrates of the pathway. Ultimately, E3s serve as crucial determinants of substrate selectivity and the timing of degradation (Hershko and Ciechanover, 1998; Yamao, 1999). Two distinct E3 families (HECT domain E3s and Ring finger E3s) have now been identified depending upon the conserved protein domains. Also, enzyme diversity (implying diversity in specificity) is apparent in E2 (Ubc), which shares the Ubc core domain that is about 30% conserved among family members. Whereas several E2s are limited to this core domain, others have significant amino- or carboxy-terminal extensions. These might facilitate

interactions with specific E3s or serve as membrane anchors with specific E3s and substrates. It has been shown that the genome of the budding yeast encodes 13 E2 products, termed Ubc1-13, and there are at least 25 mammalian family members. But not all E2s form thiol-esters with ubiquitin: Ubc9 is dedicated to sumoylation, and Ubc12 functions in rubylation. Since E2 comprises a rather small and unique family compared with E3, it can be used as a probe to survey the functional diversity of E2/E3 ubiquitin pathway in the cells. The fission yeast *S.pombe* has been used extensively as an excellent model system for the study of a highly conserved process such as chromosome segregation and genomic stability owing to its genetic tractability and similarity of its cell cycle to that of higher eukaryotic cell. Based on the domain structure known to be conserved among Ubc's, 14 Ubc's can be identified in the genome of *S.pombe* (Wood et al., 2002).

Considering the multiple roles of ubiquitin *in vivo*, it is interesting to know how ubiquitylation is implicated in the global regulation of genome integrity including mitotic recombination. In this study, I demonstrate that cells defective in Ubc7, previously designated UbcP3 (Osaka et al., 1997) (DDBJ/GenBank/EMBL/SPBP16F5.04), enhanced mitotic recombination throughout the genome. This study presents a first direct link between ubiquitylation and homologous recombination and focuses on the possible role for ubiquitylation in the negative regulation of mitotic recombination.

Results

Ubc7 is not essential for cell viability

A homology search revealed that Ubc7 is highly conserved among *S.pombe*, *S.cerevisiae*, and *H.sapiens*. They share significant amino acid homology (Fig. 3A; overall identity is approximately 60% among them). As a first step to address the cellular function of Ubc7, one copy of the *ubc7*$^{+}$ gene was disrupted in diploid strain JY765 by replacing the ORF with the *ura4*$^{+}$ gene, and correct knockout was confirmed by PCR and genomic Southern analysis. The resulting heterozygous diploid cells harboring genotype $h^{+N/-}ubc7^{+/-}$ (PY34) were sporulated and subjected to tetrad dissection. Tetrad analysis revealed that all four spores were viable and the Ura^{+} marker exactly segregated 2:2, indicating that the *ubc7*$^{+}$ gene is not essential for cell growth (Fig. 3C). Also, the *ubc7* mutant displayed no growth defect compared to the wild-type cell.

Homothallic conversion of h^{+N} heterothallism

During the tetrad analysis, I noticed a curious phenotype of $h^{+N}ubc7::ura4^{+}$ cells, the majority of which are mated zygotes and spore-forming asci, while wild-type *ubc7*$^{+}$ cells exhibited a typical haploid morphology (Fig.4B). Moreover, when these cells were further grown on EMM2 minimal medium and exposed to iodine vapor, they were positively stained with iodine despite their

haploid states, which was consistent with the microscopic features. To investigate whether this observation was all the same throughout the dissected spores, iodine staining of all the spores was employed. It was found that segregation of uracil prototrophy was tightly linked to the iodine positive phenotype, indicating that Ubc7-deficiency resulted in the phenotypic conversion leading to spore-forming ability (Fig.4A). Two possibilities could be considered in this regard. One is like *pat1* kinase mutant, which was previously reported to be proficient in haploid meiosis. This, however, was found to be not the case because further round of tetrad dissection of asci from *ubc7::ura4*$^{+}$ cells produced all four viable spores which were positively stained with iodine (data not shown). Next, the other lies on the conversion from heterothallic state to homothallic state, which is capable of switching the mating-type during mitotic growth. To address this in detail, I took advantage of a typical PCR analysis, which is widely used in determining the mating-type of the fission yeast. It revealed that *mat2-P* and *mat3-M* DNA sequences were present at *mat1* locus at approximately equal frequencies in only *ubc7::ura4*$^{+}$ cells that should be ordinarily in h^{+N} -type cells (Fig.4A, lower panel). Note that h^{+N} (*mat1*) and *ubc7* are tightly linked in this tetrad dissection. Actually, they are apart only 200-kb each other in the physical map. These results indicate that the mating-type of heterothallic h^{+N} cell was converted to that of homothallic h^{90} cell by inactivation of Ubc7.

To next confirm that this phenotype was really resulted from the Ubc7-defect, plasmid thiamine-repressible pREP81-*ubc7*$^{+}$ or empty vector pREP81 was introduced into the heterozygous diploid strain (PY34) before sporulation. The resulting recombinant strains were sporulated, and tetrad-dissected on EMM2 plate containing just adenine without thiamine to induce expression of wild-type *ubc7*$^{+}$ from *nmt* promoter. Stable Ura^{+}Leu^{+} cells were isolated, and subjected to iodine staining. Consequently, h^{+N}*ubc7*$^{-}$ cells harboring pREP81-*ubc7*$^{+}$ were not stained with iodine, clearly showing that homothallic conversion was the bona fide phenotype of Ubc7-deficiency (Fig.5B). These results indicate that h^{+N} heterothallism was converted to homothallism solely by inactivation of Ubc7. I next studied whether the homothallic conversion of h^{+N} *ubc7*$^{-}$ cells was dependent on meiotic process. This idea was confirmed by directly disrupting the *ubc7*$^{+}$ in h^{+N} haploids cells, which produced cells with the same phenotype (Fig.5A). Thus, the homothallic conversion of heterothallic h^{+N} cells was independent of the meiotic process. However, as shown in Fig.5B, Ubc7-deficiency did not stimulate the conversion of other heterothallic cells to homothallism; for example h^{-} and h^{+S} cells (see later section and Fig.2B). Therefore, Ubc7-deficiency specifically converted h^{+N} strains to homothallism. Also, I found that heterothallism, once converted from h^{+N}*ubc7*$^{-}$ cells, could not be restored even by overexpression of *ubc7*$^{+}$ from pREP81-*ubc7*$^{+}$ in these cells (data not shown). Collectively, I conclude that heterothallism of h^{+N} is irreversibly converted to homothallism due to an Ubc7-deficiency.

Homothallism and heterothallism in *S.pombe*

Homothallism is a widespread phenomenon in the fission yeast. In homothallic cell (designated h^{90} because formed about 90% spores in pure culture), the mating-type region contains three closed linked loci in the right arm on chromosome II, which extends approximately 30-kb (Fig. 2A). Their cells frequently switches mating-type by transposition of information from one of the silent donor cassettes (*mat2-P, mat3-M*) to the expressed *mat1-P/M* loci in a process similar to gene conversion (Beach and Klar, 1984a; Kelly et al., 1988). The *mat2-P* or *mat3-M* serves as a back-up library of the information of mating-type. The *P* and *M* cassettes comprise approximately the length of 1.1-kb. They are flanked by short region of homology, H2 and H1, proximal to H2. The intervening sequences between *mat1-P/M, mat2-P* and *mat3-M* are called L and K region, respectively. In addition to the h^{90} strain, several configurations of heterothallic strains were well characterized. (Fig.2B) (Beach and Klar, 1984b). h^{-S} configuration arises as a deletion by loop-out recombination between *mat2-P* and *mat3-M*, retaining a single *M* cassette in the silent region in addition to the expressed *mat1-M* cassette. This strain can no longer switch due to the absence of silent *P* cassette. h^{+S} configuration is the reverse case, which lacks *mat3-M* and retains *mat2-P* cassette. On the contrary, h^{+N} configuration results from delayed resolution of a switching intermediate during copy transposition. In the heterothallic strain, haploid cells have either a Plus(+) or a Minus(-) mating-type.

DNA rearrangement at *mat1* locus

Heterothallic h^{+N} strain has a wild-type DNA structure at the silent mating type loci (*mat2-P* and *mat3-M*) but an aberrant structure at *mat1*, in which two tandem *mat* DNA sequences (*mat1:2* and *mat3:1*) are separated by the K region, which normally lies between *mat2-P* and *mat3-M* (Fig. 2B). h^{+N} cells express only *mat1:2*(P), while the *mat3:1*(M) cassette is silent. The heterothallism, however, of h^{+N} is relatively unstable, with spontaneous production of h^{90}, wild-type homothallic cells, at the rate of 10^{-4} (Beach and Klar, 1984a; Fleck et al., 1990). This implies that the two cassettes at the *mat1* locus can be resolved by a pop-out recombination involving the H1 or H2 homology sequences. One possible explanation, therefore, for the *ubc7*$^-$-induced homothallic conversion of h^{+N} cells is the same type of recombination that occurs in spontaneous conversion, but at a greatly elevated frequency.

In order to confirm this, chromosomal DNA was prepared from $h^{+N}ubc7^+$ (JY746), $h^{+N}ubc7^-$ (PY32) and $h^{90}ubc7^+$ (PY45) strains, digested by *Hin*dIII, and analyzed by Southern hybridization. Interestingly, the 8.2- and 6.7-kb DNA bands, which are specific to $h^{+N}ubc7^+$ cells, were completely disappeared in the $h^{+N}ubc7$- cells (Fig.6A, lanes 1 and 2) and replaced with the 10.4-kb band, which stands for the normal *mat1* fragment in homothallic h^{90} cell (Fig.6A, lanes 2 and 3). These were totally consistent with the homothallic conversion observed above. Taken together, these results revealed that the *mat1* locus of $h^{+N}ubc7^-$

cells was structurally identical to that of the *mat1* in homothallic h^{90} cells and lacked tandem-duplicated DNA segments between the two cassettes.

Estimation of frequency of recombination at *mat1* locus

I have learned in the previous section that Ubc7-deficiency induced DNA rearrangement at *mat1* locus. I supposed that the mechanism of this conversion would be absolutely the same to that of the spontaneous production of h^{90} from h^{+N}, but Ubc7-deficiency may stimulate this pop-up recombination in terms of frequency. This idea was tested with determining the homothallic conversion frequency as described in *Materials and Methods*. It was estimated by measuring the loss of h^{+N}-specific DNA fragments or the appearance of h^{90}-specific DNA fragments in Southern blot. In most cases, h^{+N}-specific DNA fragments were not detectable in DNA from colonies containing $\geq 10^7$ cells (*i.e.* that had passed through more than 24-25 cell divisions) that originated from a dissected $h^{+N}ubc7^-$ spore (Fig. 7A, lanes 1 and 4). The simulation revealed that the rate of homothallic conversion at *mat1* in $h^{+N}ubc7^-$ cells was on the order of 10^{-1}, which is extraordinarily high compared with the 10^{-4} of the spontaneous appearance of h^{90} in $h^{+N}ubc7^+$ cells (Fig 7B). Taken together, I conclude that Ubc7-defect resulted in the elevated level of recombination at *mat1* locus by the

order of 10^{-1}, which may be meaningfully comparable to that of mating-type switching, which is a highly programmed cellular event.

Effect of *smt* on *mat1* rearrangement and homothallic conversion

Mating-type switching is initiated by DSB between the *mat1* cassette and the H homology box in switching-competent cells (Arcangioli, 1998; Klar and Miglio, 1986). This DSB is generated by rather complex mechanism, which involves a strand-specific imprinting in the previous cell cycle (Arcangioli and de Lahondes, 2000; Dalgaard and Klar, 1999; Dalgaard and Klar, 2000). The biochemical and molecular nature remain not fully understood, but it requires the *cis* element *smt*, located at the distal end of H1 region of *mat1*. The *smt-0* mutant allele, a 270-bp deletion from DSB site, was previously reported to be completely defective in the generation of DSB and subsequent mating-type switching (Nielsen and Egel, 1989; Styrkarsdottir et al., 1993).

In order to study whether the homothallic conversion of h^{+N} requires the *smt*-dependent DSB, I attempted to construct an h^{+N}*smt-0* strain that also contains *ubc7* allele. The strategies for construction were as follows; h^{-}*smt-0* cells (PY119) were transformed with PCR-amplified fragments containing sequences from upstream of *mat1:2* through the middle of the *mat3:1* cassette of h^{+N} cells, excluding the *smt* site. The resulting transformed cells were placed on

sporulating medium for four days, and spores that survived from glusulase (snail juice-enzyme) treatment were selected. h^{+N} cells and *smt-0* deletions were confirmed through PCR screening, and then *ubc7* mutation was introduced in this h^{+N}*smt-0* background, generating h^{+N}*smt-0ubc7*$^{-}$. To next address the *smt* effect, five sets of strains (h^{+N}*ubc7*$^{+}$, h^{+N}*ubc7*$^{-}$, h^{+N}*smt-0ubc7*$^{+}$, h^{+N}*smt-0ubc7*$^{-}$, h^{90}*ubc7*$^{+}$) were grown in YES medium. Then, chromosomal DNA from each strain was isolated, digested with *Hin*dIII, and subjected to Southern analysis. As a result, no DNA rearrangement was observed in this *smt-0* background even though Ubc7 was inactivated (Fig. 8A, lanes 3 and 4; *smt*$^{+}$ control, lane 2). Also, the microscopic features of the cells and iodine staining indicated the lack of homothallic state of h^{+N}*smt-0ubc7*$^{-}$ cells (Fig. 8B, lanes 3 and 4). These results strongly indicate that the DNA modification and the subsequent DSB at *mat1*, which are induced depending on the *smt* function, is essential not only for mating-type switching but also for homologous recombination event induced by Ubc7-defect.

No significant increase of recombination frequency at *ade6* locus

I next studied whether Ubc7-defect would also affect the enhancement of mitotic intrachromosomal recombination in addition to the *mat1* locus. The purpose of this experiment describes whether Ubc7^{-}-induced recombination has a

general effect throughout whole genome or not. Strain containing tandem direct repeats of *ade6* heteroalleles with a functional *ura4*$^+$ gene between the repeats was employed to study the intrachromosomal recombination by the recovery of Ade$^+$ recombinants (Fig. 9A). Two main classes of Ade$^+$ recombinants can be distinguished; Ade$^+$Ura$^-$ crossing-over type recombinants and Ade$^+$Ura$^+$ gene-conversion types.

To test this, I directly disrupted the *ubc7*$^+$ gene by using the *G418* module in strain PS1 harboring the *ade6-M26* mutation (Schuchert and Kohli, 1988), which is shown to be a meiosis-specific recombination hotspot. Then, Ade$^+$ reversion rate was determined for *ubc7*$^+$ and *ubc7*$^-$ cells. However, I did not found significant differences between two types of strains; Ade$^+$ recombinants in both strains arose at average rates of $0.9\text{x}10^{-4}$ and $1.0\text{x}10^{-4}$ per cell division, respectively (Fig. 9B). Furthermore, about 45% of these recombinants were found to be conversion-types and remainders were crossing-over types. Provided with these results, I thought that Ubc7-deficiency *per se* did not affect the recombination between this *ade6* duplication. This result was not consistent with the elevated recombination at *mat1* locus only after inactivation of Ubc7. Based on these findings, I speculated that any structural differences may occur at two different loci of *mat1* and *ade6*.

Mat1 locus is known to be intrinsically competent for recombination required for the mating-type switching. Supporting this, I found in the previous

study that the *smt* deletion induced neither homothallic conversion nor DNA rearrangement at *mat1* locus, showing that Ubc7$^-$-induced recombination is thoroughly dependent on recombinogenic DNA state. On the contrary, at least *ade6* duplication itself has no structural characteristic corresponding to DSB or its equivalent. To examine this possibility, I tried to introduce a similar structure to that of *smt* at *mat1* locus into the tester strain.

Effect of UV irradiation on mitotic intrachromosomal recombination

UV irradiation has long been known to stimulate mitotic recombination in a variety of organisms (Osman et al., 2000). It has been previously shown to stimulate interchromosomal mitotic recombination in *S.pombe* (Grossenbacher-Grunder and Thuriaux, 1981). I speculated whether UV irradiation could also act as an exogenous DSB generator. This idea was tested by monitoring Ade$^+$ reversion rate between *ubc7*$^+$ and *ubc7*$^-$ cells upon UV irradiation at dose of 100 J/m^2. As shown in Table 2, both *ubc7*$^+$ and *ubc7*$^-$ cells efficiently produced Ade$^+$ recombinants compared with their unirradiated controls. The *ubc7*$^+$ cells had a 3.7-fold and *ubc7*$^-$ cells had a 4.7-fold, respectively. Also, particularly, the rates of Ade$^+$Ura$^+$ were increased in both strains by 1.8 and 2.0-fold, respectively.

Although increased reversion rate was observed in *ubc7*$^-$ cells compared with *ubc7*$^+$ cells upon UV irradiation, the degree of increase is rather ambiguous (The rate of Ade$^+$ reversion for *ubc7*$^+$ and *ubc7*$^-$ cells was $3.3\text{x}10^{-4}$ and $5.0\text{x}10^{-4}$, respectively). Hence, why could not Ubc7-defect drastically induce enhanced recombination upon UV irradiation? One possibility is that UV dosage used might be so weak not to be optimized for creating circumstances favoring mitotic intrachromosomal recombination. In other words, roles of Ubc7-defect in recombination could be severely diminished under this condition. It is likely that UV irradiation could induce rather complex reaction products that could not be yet fully explained. For example, not only DSB formation, but also DNA strand exchange might be induced by UV irradiation. Although I cannot think these results conclusive, they may argue the following points; the increased rates of recombinants, though not drastic increase, and the differential effects on the types of recombination suggest that recombination mechanisms, particularly those causing Ade$^+$Ura$^+$ recombinants, might contribute to UV damage-induced repair and thus survival in cells. As a next try to introduce DSB, an endogenous Rad2-defect was induced.

Drastic increase in mitotic recombination entailed by *rad2* mutation

I next introduced the *rad2* mutation into tester strain to mimic a DSB-like structure at *ade6* locus. Rad2 is a *S. pombe* counterpart of *S.cerevisiae* Rad27 and mammalian FEN-1 (flap endonuclease/five prime exonuclease) (Alleva and Doetsch, 1998; Murray et al., 1994). A subgroup of FEN-1 family is shown to have a 5'→3' exonuclease activity essential for the completion of lagging strand DNA synthesis. Okazaki fragments are ligated together through a process called Okazaki fragment maturation, which requires the combined action of FEN-1, RNase H1, and DNA ligase I. The deletion of *rad2* in *S.pombe* increased the rates of spontaneous mutation, mitotic recombination, and chromosome loss, consistent with it the critical roles for chromosome maintenance. Also, it has been reported that *rad2* mutants accumulate DSBs during replication fork arrest and that these DSBs are repaired by homologous recombination.

To address the Rad2-defect in the intrachromosomal recombination, all the isogenic strains carrying the *ade6* heteroalleic duplications, *ubc7*$^{+}$*rad2*$^{+}$ (PY55), *ubc7rad2*$^{+}$ (PYK62), *ubc7*$^{+}$*rad2*$^{-}$ (PY74), and *ubc7rad2*$^{-}$ (PY76) were constructed and then subjected to Ade^{+} recombination assay (Table 3). As previously reported, *rad2*$^{-}$ cells are more recombinogenic than wild-type cells and accordingly, *rad2* mutation produced Ade^{+} recombinants at a higher rate than wild-type cells. The simultaneous *ubc7* mutation in *rad2*$^{-}$ background caused a

drastic increase in the rate of Ade^+ reversion. The *ubc7 rad2*$^-$ cells had a 3-fold higher rate of reversion than *rad2*$^-$ cells and 11-fold higher rate than wild-type or *ubc7* single mutant. These results may suggest that Ubc7-defect enhances the general recombination activity that functions after cells produce the recombinogenic DNA essential for the initiation of the DNA strand exchange event.

Also, the majority of the increased Ade^+ recombinants seen in response to *rad2* mutation was Ade^+Ura^-, and thus resulted from crossing-over (The increased ratios of Ade^+Ura^- and Ade^+Ura^+ were 5.5 and 1.8, respectively). In the *rad2*$^-$ background, Ubc7-deficiency induced recombination by 15.4 and 6.6 fold for Ade^+Ura^- and Ade^+Ura^+, respectively, and thus the fold increases of Ade^+ Ura^- and Ade^+Ura^+ due to the *ubc7* mutation were calculated to be 2.8 and 3.7, respectively. Taken together, this indicates that Ubc7-deficiency stimulated the production of both Ade^+Ura^- and Ade^+Ura^+, about equally, in contrast to the stimulation of a particular type of recombination by mutations such as a Rad2-defect.

Increased DNA repair activity

The fact that Ubc7-deficiency induced the elevated recombination led me to speculate the effects of Ubc7-deficiency on the increased DNA repair activity in

the cell. Hyper-recombination has been often related to genomic instability, which is generally accompanied by increased sensitivity to various types of DNA damage. I, therefore, examined whether *ubc7* mutants were defective in DNA repair. Surprisingly, *ubc7*$^-$ cells (PY32) were substantially more resistant to UV irradiation and MMS than *ubc7*$^+$ cells (JY746) (Fig. 10A and B). Furthermore, the increased DNA repair activity was completely dependent on *rhp51*$^+$, since *rhp51*$^-$*ubc7*$^-$ double mutant (PYK60) and *rhp51*$^-$ single mutant cells (PY64) were equally sensitive to DNA damage (Fig. 10C). These results strongly suggest that the increased DNA repair activity of the *ubc7* mutant was due to the increased recombination repair activity by itself, and not to some indirect effect via the production of recombinogenic DNA as a result of the decreased genomic stability. In other words, Ubc7 negatively regulates cellular activities of homologous recombination and recombination repair in the cell.

Enhanced recombination at rDNA repeats

In most eukaryotic organisms, the genes for rRNA are clustered in long tandem repeats on one or a few chromosomes. The total number of these chromosomal rDNA repeats appears to be maintained at a level appropriate for each organism. *S.pombe* rDNA repeats consist of 100-150 copies (10.9-kb tandem head-to-tail repeats) in two large clusters at both ends of chromosome III

(Maleszka and Clark-Walker, 1993; Mizukami et al., 1993). The unit of rDNA repeat consists of a transcription unit for 35S rRNA precursor (ETS; 7.9-kb) and a nontranscribed spacer (NTS; 3.0-kb), which contains promoters and other regulatory sequences.

In *S.cerevisiae*, the origin of replication (*ARS*) and the replication fork barrier (*RFB*) sites are located in NTS region. The *RFB* site contains a specific nucleotide sequence of~100 bp that allows progression of the replication fork in the direction of 35S rRNA transcription, but not in opposite direction. It has been suggested previously that the *RFB* site might have evolved to prevent collision between the transcription and replication machineries. The pausing of DNA replication machinery at the *RFB* site stimulates DSB formation, perhaps in the sister chromatid with newly synthesized lagging DNA strands. There are some reports that rDNA expansion/contraction would be regulated by changing *in vivo* recombination activity such as in *FOB1* deletion, which was previously shown to be required for replication fork blockage at *RFB* site (Kobayashi et al., 1998; Kobayashi and Horiuchi, 1996). However, there is no strong evidence(s) for the control mechanism of rDNA repeats in *S.pombe*. Given that Ubc7 could negatively regulate cellular activities of homologous recombination, it is very interesting to study whether recombinogenic abilities induced by Ubc7-defect would have any influence(s) on the recombination at rDNA cluster, in which occurs naturally, unlike the artificially constructed *ade6* duplication.

In order to address this possibility, PFGE was employed as described in *Materials and Methods*. When $h^{+N}ubc7^{+}$ (JY746), $h^{+N}ubc7^{-}$ (PY32), $h^{90}ubc7^{+}$ (JY878), and $h^{90}ubc7^{-}$ (PY45) cells were subjected to PFGE analysis, the electrophoretic migration of chromosome III only in *ubc7*$^{-}$ cells was retarded than that of *ubc7*$^{+}$ cells, both in h^{+N} and h^{90} strains (Fig. 11B, upper panel; lanes 3/4 and 5 compared to lanes 1 and 2). Furthermore, Southern blot analysis revealed that in *ubc7*$^{-}$ cells, the intensity probed with DNA sequences encoding 18S rRNA were stronger than that of *ubc7*$^{+}$ cells (Fig. 11B, lower panel; lanes 3/4 and 5 compared to lanes 1 and 2). These results strongly suggest that the increase of rDNA copies was induced by Ubc7-defect. Provided that the Ubc7-defect induced enhanced recombination at rDNA repeats, all my findings were wholly consistent with those in *S.cerevisiae*.

Partial impairment in transcriptional silencing

Several reports strongly argued that components of the ubquitin pathway are involved in heterochromatin silencing (Choi et al., 2002; Huang et al., 1997; Nielsen et al., 2002; Singh et al., 1998). Deletion of *UBP3*, which encodes a deubiquitin enzyme, increased silencing at both the telomere and *HML* locus. Mutation of *S.cerevisiae RAD6* disrupted silencing at telomere and *HM* loci. *S.pombe rhp6* (*RAD6* orthologue), *ubc15* and *ubcx* have been previously reported

to affect transcriptional silencing, suggesting their redundant roles. Despite these observations, the molecular mechanism for regulating silencing is yet unclear. The fact that Ubc7-deficiency caused the enhanced recombination argues the possibility that recombinogenic state could be brought about by the alteration of chromatin structure, probably increasing DNA access by recombination protein complexes. The chromatin remodeling has been often related to transcriptional silencing, which is a specialized mechanism that depends on the establishment and maintenance of repressed or silenced chromatin. With this in mind, it is interesting to study whether Ubc7-defect would affect transcriptional silencing in the heterochromatin region.

To address this possibility, the reporter gene *ade6*$^{+}$ inserted in the right side of the *otr1R* locus of *cen1* was employed to detect changes in *otr1* locus repression by monitoring the color of colonies. The tester strain FY1193 also carries the *ura4*$^{+}$ marker in the left side of the *imrL* locus. During a series of analysis, I found an interesting phenotype that *ubc7*-knockout strain (PYK52) exhibited some heterogeneity of the color of colonies, in which red and light pink (or sectored colonies) were simultaneously observed. I supposed that this heterogeneity was probably resulted from the mixture of red (repressed state) and white (de-repressed state) colonies. Indeed, within the population, 10-20% of colonies were found to be light pink and the remainders were mainly red, while the tester strain only produced red colonies due to its silence state (Fig.12A,

ubc7$^+$ and *ubc7*$^-$). Moreover, when cells from a pink *ubc7*$^-$ colony were re-streaked immediately on YE plate, about 85-90% of progeny colonies remained pink, indicating a relatively stable inheritance (Fig.12A, *ubc7*$^-$*-pink*). On the other hand, the conversion from red to pink was completely suppressed upon the transmittable expression from pREP41-*ubc7*$^+$, which carries wild-type *ubc7*$^+$ allele (Fig.12A, *pREP41-ubc7*$^+$). Consecutively, when the plasmid pREP41-*ubc7*$^+$ was segregated-out by further rounds of re-streaking cells on nonselective plate, pink colonies were reappeared by an order of original yield (approximately 10-20%), showing an authentic phenotype induced by Ubc7-defect (Fig. 12A, *segregated-out*). These results suggest that Ubc7-defect might entail a partial loss of transcriptional silencing.

However, I could not find the same phenotype in the reporter gene *ura4+* inserted in the left side of the *imrL* locus (Fig. 12C). Both *ubc7*$^+$ and *ubc7*$^-$ cells displayed no discernable effect on the silencing on the *imrL* locus since both cells grew well on uracil-free or counterselective FOA plates regardless of Ubc7-function, showing a leaky expression of *ura4*$^+$ gene. This probably means that the tester strain itself carries a weakly silenced copy of the *ura4*$^+$ gene contrary to the *ade6*$^+$ gene. However, I could not exclude the possibility that the loss of silencing caused by Ubc7-deficiency might occur in a site-specific manner. In order to test this possibility, a reverse configuration (i.e. *imrL::ade6*$^+$ and *otrR1::ura4*$^+$) should be absolutely required. Although these observations are

preliminary and not yet convincing, it is possible that Ubc7-mediated ubiquitylation might affect transcriptional silencing such as previously reported other Ubc's.

Ubiqutin ligase : Pcu3 as a possible candidate

The E3s play most crucial roles in determining the timing and specificity of ubiquitylation, but the least well understood. This is because, in contrast to E2s, different E3 families share little or no homology among each other, and also because E3s are in low abundance in the cells. Some E3s are composed of large number of subunits, but in many cases the basic function of each component is largely unknown. Keeping this in mind, it is very worthy to survey for an E3 functioning in the regulation of mitotic recombination. One group has previously reported that the RING protein Pip1, *S.pombe* homologue of *S.cerevisiae* Rbx1/Hrt1/Roc1, could physically interact with several Ubcs including Ubc7 through a series of biochemical studies (Zhou et al., 2001). Also, *in vitro* ubiquitylation assay with a tagged version of Pcu3, *S.pombe* counterpart of human CUL-3, showed that efficient formation of polyubiquitin chain was specific for Ubc7 among the 14 Ubc's identified in *S.pombe*.

Based on the previous report, I thought the possibility that Ubc7 and Pcu3 might have similar function *in vivo*. In order to address this, one copy of the

pcu3$^+$ gene was disrupted in the diploid strain, and its correct knockout was verified by genomic Southern analysis (Fig. 13A). Through tetrad analysis of the heterozygous diploid, the *pcu3*$^+$ gene was found to be nonessential and *pcu3*$^-$ cells showed no growth disadvantages compared to wild-type cells. (Fig.13B). My finding, however, was contradictory to the previous report (Kominami et al., 1998). They showed that *pcu3*$^-$ cells displayed severe growth defect compared to wild-type cells, though the *pcu3*$^+$ gene was not essential, since two normal sized-colonies (wild-type) and two tiny colonies (*pcu3*$^-$) were observed in the tetrad dissection. However, I could not find such a growth-defective phenotype even though after new round of disruption of *pcu3*$^+$ gene, probably suggesting their wrong disruption (the result from another group supports my finding). Anyway, I next examined the response of *pcu3* mutation with respect to DNA damage. Interestingly, it was found that the *pcu3*$^-$ cells were substantially more resistant to UV and MMS-induced DNA damage than wild-type strain, consistent with those of the *ubc7*$^-$ cells. (Fig.13C and D). Thus, this result strongly suggests that Pcu3 may function as an E3 for Ubc7 in the global regulation of mitotic recombination. Whether or not Pcu3-deficiency would enhance mitotic recombination in concert with Ubc7 is currently under progress.

Discussion

Most eukaryotic organisms have defense mechanisms to protect them from environmental stresses such as mutation and DNA damage, otherwise lead to genomic instability and subsequent cell death (Pickart, 2001). Although homologous recombination has to be strictly regulated to maintain genome integrity, the molecular mechanism for this regulation remains still poorly understood. In the current study, I reported several lines of evidence indicating that Ubc7, one of the 14 Ubc's, negatively regulates mitotic homologous recombination and recombination repair in the fission yeast. Some type of genetic elements which elevate recombination frequencies are known, including *ade6-M26* hotspot in *S.pombe* and *Chi* sequences in *E.coli* and phage lambda (Alleva and Doetsch, 2000). In these cases, the element functions in *cis* in a site-specific manner, inducing enhanced initiation of recombination nearby. On the contrary, the *ubc7* mutation described herein influences recombination in *trans*-manner because enhanced recombination took place in *ubc7*$^-$ cells at two different loci, *ade6* and *mat1* loci, located independently of the *ubc7* gene.

Firstly, I found an attractive phenotype that *ubc7* mutation resulted in increased homothallic conversion of h^{+N} heterothallism (Fig. 4 and 5). Other heterothallic types, h^{+s} or h^-, in which *mat3-M* and *mat2-P* is deleted, respectively, were not converted to homothallism even though Ubc7 was inactivated. Mating-type switching of the fission yeast is a highly regulated

DNA recombination event that occurs in a homothallic cell. Two consecutive asymmetric divisions are required to produce one mating-type switched cell among the four progeny (so-called one-in-four rule). The h^{+N} heterotahllic cell can be produced from h^{90} homothallic cell by a rare aberrant switching event at frequencies of 10^{-4} (Beach and Klar, 1984a). In turn, a heterothallic cell can also revert to a homothallic cell by DNA rearrangement at the *mat* locus. I showed here that the *ubc7* mutation in h^{+N} configuration promoted to pop-out the tandem-duplicated segments at the *mat1* locus, inducing the DNA rearrangement structurally identical to that of h^{90} configuration (Fig. 6). Also, the simulation results showed that the conversion frequency by *ubc7* mutation was remarkably high (10^{-1}) compared to that of spontaneous conversion (10^{-4}), suggesting that this conversion may be comparable to a highly programmed mating-type switching event (Fig. 7). At least, these findings describe the first evidences that stimulate the recombination to produce an h^{+N} type from h^{90} type in terms of accelerated conversion frequency (about 1,000-fold increase).

Mating-type switching is initiated by DSB. Recent molecular mechanisms revealed that the presence of a site- and strand DNA-specific break or DNA modification at the *mat1* locus which prepares the switching event during the next round of DNA replication, strongly supporting the concept that DNA replication and recombination at *mat1* are highly coupled (Arcangioli, 1998; Arcangioli and de Lahondes, 2000). It requires the *cis* element *smt*, located

near the H1 homology sequence in *mat1*. The role of *smt* in rearrangement of *mat1* in *ubc7*⁻ cells was examined. In a heterothallic h^{+N}*smt-0ubc7*⁻ strain, neither homotahllic conversion nor *mat1* rearrangement was found (Fig. 8). Thus, DNA modification at *mat1* is required for homologous recombination at *mat1* locus as well as for mating-type switching

Hyper-recombination phenotype has been reported in few cases thus far. Without exception, however, mutants showing hyper-recombination activities are defective in repair of DNA damage associated with a genomic instability, generating an increased sensitivity to DNA damage. Inactivation of, for example, *rad2* or *rqh1hus2/rad12*, *S.pombe* orthologue of *S,cerevisiae Rad27* or Sgs1 (ATP-dependent *RecQ* type DNA helicase), respectively, confers hyper-recombination together with an increased sensitivity to DNA damage (Grossenbacher-Grunder and Thuriaux, 1981; Stewart et al., 1997). However, I showed here that the *ubc7* mutant displayed both hyper-recombination and hyper-resistance to DNA damage (Fig.10). To our knowledge, this is an unreported and quite novel phenotype in itself. Moreover, the increased resistance to DNA damage in *ubc7*⁻ cells was found to be completely dependent on the function of Rhp51, *S.pombe* counterpart of *S.cerevisiae* RAD51. It could be suggested that the DNA repair activity of the *ubc7* mutant was increased due to the increased recombination repair activity *per se*, but not to the indirect effect by the production of recombinogenic intermediates through a decreased genomic

instability. It also means that Ubc7-deficiency causes a hyper-recombinogenic state throughout whole genome in the fission yeast

The *ade6-M26* mutation is a well-defined hotspot for meiotic recombination that is initiated by DSB near the mutation site (Szankasi et al., 1988; Young et al., 2002). However, Ubc7-deficiency did not affect the recombination at *ade6* duplication containing an *ade6-M26* mutation (Fig. 9). Thus, the *ade6-M26* mutation was not recombinogenic during mitotic division in *ubc7*$^-$ cells, indicating that Ubc7-deficiency did not mimic DSB creation during the mitotic process. Interestingly, the recombination at *ade6* duplication was drastically enhanced when the concurrent *rad2* mutation was introduced into the *ubc7* mutant. Rad2-defect is previously shown to induce the recombinogenic state due to an incomplete processing of Okazaki fragment, indicating a role in the production of recombinogenic DNA structure. I found that the strain carrying the double mutation of *ubc7* and *rad2* exhibited a higher rate of recombination than that of each single mutant (Table 3). These results are consistent with those of *smt-0* deletion, in that ubc7$^-$-induced recombination is absolutely dependent on the recombinogenic DNA state caused by DSB.

The *ubc7* defect enhanced both gene conversion (Ade^+Ura^+) and pop-out (Ade^+Ura^-) recombination equally, since the proportion of the two modes of recombination between the *ade6* heteroalleic duplication was not affected by the *ubc7* mutation (Table 3). Provided that the mode of recombination is affected

by resolution polarity in recombination intermediates, the results presented here suggest that *ubc7*-mediated ubiquitylation might exert control over middle step following the DNA exchange and preceding the resolution reaction, a final step of recombination. In contrast to Ubc7-defect, Rad2-defect stimulated the pop-out reaction markedly than gene conversion reaction. These findings strongly suggest that Rad2 and Ubc7 function at distinct stage during homologous recombination. This indicates that Ubc7-defect does not cause increased production of recombinogenic DNA. The fact that the hyper-recombination in *ubc7* mutant requires *smt-0* or *rad2* mutation also suggests that inactivation of Ubc7 does not stimulate the DSB formation that occurs in the initiation step of homologous recombination.

I observed enhanced recombination at *ade6* and *mat1* loci. One question can arise in this step. Why does Ubc7$^-$-induced recombination occur at a different order in two different loci? This may not indicate site-specificity but rather that there is some difference in the structure or degree of DNA competence for recombination induced by the two different ways. *smt*-dependent DNA modification at *mat1* may be quite efficient because it is tightly associated with cell-cycle program of mating-type switching. The fact that the pop-out recombination frequency at *mat1* locus was increased up to a level comparable to that of mating-type switching may indicate that interference with recombination might be totally abolished in *ubc7*$^-$ cells, generating a favorable circumstance(s)

for recombination. Mating-type switching in *S.pombe* requires site-specific recombination mainly driven by specific recombination machinery including *swi* gene products, although it also needs, at least in part, the assistance of the general recombination apparatus. Therefore, it could be argued that the products of some *swi* genes might stimulate homologous recombination using H1 and H2 sequences at *mat1* but not *ade6* in *ubc7* cells. In contrast, DSBs or their equivalents induced by Rad2-deficiency would be located in the *ade6* region without time and site specificity. Thus, it is possible that DNA competence induced by Rad2-deficiency might be bottleneck or liming-step of the recombination frequency.

In addition to *mat1* and *ade6* loci, Ubc7-defect enhanced recombination at rDNA repeats that govern the two-third of chromosome III in *S.pombe*. PFGE and Southern analysis revealed that chromosome III in *ubc7* mutant was slowly migrated than that of wild-type strain, indicating a direct evidence for the increase of rDNA copies (Fig. 11). At least until far, there are no strong evidences for the control mechanisms of rDNA repeats in *S.pombe*. On the contrary, *S.cerevisiae FOB1*, which is shown to be required for replication fork blockage and recombination hotspot (*HOT1*) activity, plays a role in rDNA expansion and contradiction. There is one putative counterpart of *FOB1* in the genome of *S.pombe* (AL109831). It is possible that future elucidation of this

protein together with Ubc7-function will make it clear how the total number of chromosomal rDNA repeats is stringently regulated in *S.pombe*.

Chromatin-based epigenetic imprints contribute to maintenance of higher order chromatin structure, which controls transcriptional silencing at silent loci (Grewal et al., 1998; Grewal and Elgin, 2002). I showed here that a mutation defective in Ubc7 gave rise to a partial loss for suppressing variegation of marker gene inserted into the *otr1* region in centromere, suggesting a potential role of Ubc7 in transcriptional silencing (Fig. 12). There are some emerging reports that several Ubc's may be involved in transcriptional silencing although their molecular mechanisms remain not fully understood. Based on my observation that Ubc7-defect caused a partial loss of silencing, it also argues the possibility that Ubc7-mediated ubiquitylation might modify or degrade some regulator proteins (for example, inhibitor of methylase or deactylase) that control activities or functional roles of direct components essential for heterochromatin assembly, such as Swi6, Clr3, Clr4, and Rik1 proteins. It will be also interesting to investigate the recruitment of these proteins to the heterochromatin region with respect to Ubc7-function

What is (are) the target(s) of Ubc7-mediated ubiquitinylation? The classical role of ubiquitylation is that it targets abnormal proteins for proteosomal degradation, but recent findings suggest that it may also have other functions such as regulation of protein activity. The most obvious such target(s) would be

Rhp51 and/or Rad22. They are highly conserved recombination proteins and play major roles in genetic recombination. *S. pombe* Rad52 has been shown to be modified by SUMO. Human Rad51 is also sumorylated *in vitro*. Thus, this protein might also be ubiquitylated, as suggested by the recently reported competitive modification by SUMO and ubiquitin at the same lysine residue of PCNA (Hoege et al., 2002). The second-most obvious candidates are mismatch repair proteins. It has been shown that mismatch repair proteins work as a barrier against homologous recombination in both bacteria and eukaryotes, and that they inhibit RecA-catalyzed strand exchange *in vitro* (de Wind et al., 1995; Rayssiguier et al., 1989; Worth et al., 1994). A third type of candidate is chromatin-related protein such as histone or heterochromatin proteins. Ubc7-deficiency may lead to chromatin remodeling and increased access to DNA by recombination protein complexes.

Ubc7 in *S. pombe* seems to be a homologue of Ubc7 in *S. cerevisiae*, since these proteins share the highest homology in primary structure among the Ubc's in the two species. In *S. cerevisiae*, Ubc7 forms a complex with Ubc6 and is involved in degradation of the *Mat2* transcriptional regulator (Chen et al., 1993). Ubc7 also confers stress- and cadmium-resistance on *S. cerevisiae* (Hochstrasser, 1996). A proposed structural homologue in mammalian cells, such as UbcH7 in human cell, is localized in the endoplasmic reticulum (ER) in connection with ERAD (ER-associated degradation) (Sommer and Wolf, 1997). However, the

common physiological function of the three Ubc7's has not been determined, although the ubiquitin system is widely conserved among eukaryotes. Thus, it is possible that the regulation of homologous recombination by Ubc7 is also a widely conserved phenomenon in many organisms.

The cullin/RING family of E3 comprises a multifunctional set of enzymes controlling the stability and activity of various cellular events (Deshaies, 1999). Among the best-studied examples of cullin/RING enzymes are so-called SCF complexes. SCF complexes share homologues of the core component cullin-1 (CUL1), Skp1, and the RING domain protein, which associates with different F-box proteins and Ubc's. *S,cervisiae* Cdc53, *S.pombe* Pcu1, and human CUL1 has been shown to be a scaffold protein of SCF complex. In addition to CUL1, the human genome has at least five other cullins, CUL2, 3, 4A, 4B, and 5. This diversity is partially conserved in *S.pombe*, which encodes *pcu3* and *pcu4,* homologues of human CUL3 and CUL4, for which there are no direct orthologues in *S.cerevisiae*. It has been shown that all human cullins interact with the Hrt1/Rbx1 RING protein (Ohta et al., 1999) and has ubiquitin ligase activity *in vitro* (Ohta and Xiong, 2001). I showed that deletion of *pcu3* caused the hyper-resistance to DNA damage such as UV and MMS (Fig.13B and C). This result was consistent with that of Ubc7-defect, strongly suggesting that Pcu3 may function as an E3 for Ubc7. In addition, there are some arguments that cullin families in *S.pombe* may be implicated in the repair and tolerance

mechanisms of DNA damage; Pcu1 (checkpoint) (Mundt et al., 2002), Pcu4 (base excision repair), Pcu3 (recombinational repair; this study). The functional characterization of Pcu3 should be absolutely required in connection with recombination. In addition to E3, the identification of the protein targets of Ubc7-mediated ubiquitinylation in the future will reveal the mechanism by which Ubc7 represses homologous recombination. The present study represents the first step toward understanding the global regulation of mitotic recombination by ubiquitylation in the fission yeast.

MATERIALS AND METHODS

Strains, media and genetic techniques

The *S.pombe* strains constructed and used in this study are listed in Table 1. *S.pombe* cells were maintained and grown in the following media; yeast extract medium (YE), yeast extract supplemented (YES) or Edinburgh minimal medium (EMM2) supplemented with appropriate nutrients. For long-term storage, cells were kept at –80C as 25% glycerol stocks, if necessary, they were activated on an appropriate plate for short-term usage. *S.pombe* cells were transformed via the lithium acetate method. The experiments of conjugation and sporulation were performed on malt extract plate (ME) or spoulation plate (SPA). The homozygous diploid strains were constructed by cell fusion. Standard genetic tools including tetrad dissection were performed as described elsewhere (Alfa et al., 1993; Moreno et al., 1991). *S.pombe* cultures were routinely incubated at 30°C otherwise stated. *E.coli* DH5 was used for cloning plasmids. It was usually propagated in Luria broth. Ampicillin or kanamycin was used at a final concentration of 100 μg/ml or 50 μg/ml, respectively.

Iodine reaction and DAPI staining

Homothallic and heterothallic cell of *S.pombe* can be distinguished on sporulation medium or minimal medium by staining cells with iodine vapor.

Since only spores contain starch, homothallic colonies turn homogeneously brown (iodine positive), while the non-sporulating heterothallic colonies are yellow (iodine negative). *S.pombe* cells were usually grown to saturation on EMM2 or SPA plates, and then exposed to iodine vapor before being photographed. In order to investigate the nuclear structure, DAPI (4,6-diamidino-2-phenylindole) was used to stain the cells. *S.pombe* cells were harvested, washed, mixed with DAPI/antifade solution, and subjected to fluorescence microscopy.

Plasmid construction

Standard molecular biology techniques were followed as previously described. Restriction enzymes and DNA modifying enzymes were used as recommended by the suppliers (mainly purchased from Takara Shuzo and Toyobo Biochemicals). The PCR was carried out under the best-optimized condition by using DNA Thermal Cycler480 (Perkin Elmer Ltd.). For southern analysis, the thermostable alkaline phophatase system was used to label DNA probes (Amersham Pharmacia Biotech). If required, cDNA for each gene was isolated from *S.pombe* total RNA by reverse transcription. For bacterial expression of *ubc7*$^{+}$ gene, the appropriate restriction enzyme sites were introduced by PCR before and after the coding sequence, and then ligated to in frame to the pRSETA vector harboring T7 promoter, yielding pRSET-*ubc7*$^{+}$. In order to construct of a series of *ubc7*$^{+}$ versions under the control of thiamine-

repressible *nmt* promoter functioning in *S.pombe*, several oligonucleotides were used to amplify the *ubc7* cDNA by PCR. The amplified DNA fragments were digested by restriction enzymes *Nde*I and *Bam*HI, and subcloned into a series of pREP vectors, generating pREP1, 41, 81-*ubc7*$^+$.

Gene disruption

Gene disruption was performed by one-step gene replacement. The DNA sequences immediate upstream (-398 to +1) and downstream (+943 to +1603) of the *ubc7*$^+$ ORF were amplified by PCR using wild-type genomic DNA (isolated from JY741) as a template with a pair of primers Ubc7-N (5'-CCC GAA TTC CAT TGT GAT ACA TCC, *Eco*RI restriction site is underlined) and Ubc7-C (5'-TAT AAG CTT TGG AAG CGG GAG GTG, *Hin*dIII restriction site is underlined). Using the restriction sites at the ends, the PCR products was cloned into the BS-*ura4*$^+$, which is a derivative of pUC119 vector containing a 1.8-kb *ura4*$^+$ fragment. The resultant plasmid pUP3 was digested by *Hin*cII and *Xba*I to release the *ubc7*$^+$*::ura4*$^+$ fragment and used to transform *ura4D-18* strains including diploid stain JY765. Alternatively, if necessary, *G418* module (Bahler et al., 1998) was used instead of an *ura4*$^+$ fragment. A set of primers Ubc7-N1 (5'-TCC AAT TGC ACT CGG ATA CG-3') and Ubc7-C1 (5'-TTT GGA GCA TAA TTT GGG GTT A-3') were used to confirm the correct disruption. Also, *rad2*$^+$ or *pcu3*$^+$ gene was knock out by replacing each ORF with a 2.3-kb *LEU2*$^+$ or 1.8-kb *ura4*$^+$ fragment, respectively.

Identification of *mat1* sequences by PCR

Cells were picked up from a given colony and suspended in 10 μl of zymolase-100T solution (3 mg/ ml in 5x TE). After incubation for 1 hr at 37°C, and then for 5 min at 100°C, 1 μl of the suspension was used as a template in a standard PCR reaction with a mixture of the following three primers; *mat1*,5'-AGAAGAGAGAGTAGTTGAGAG3';*mat2P*,5'ACGGTAGTCATCGGTCTTCC-3';*mat3M*,5'-TACGTTCAGTAGACGTAGTG-3'. The PCR amplification of the *mat1-P* and *mat1-M* sequences produced 0.9- and 0.7-kb DNA fragments, respectively.

Southern blot analysis and Pulse-field gel electrophoresis

For Southern blot analysis of *mat1* locus, chromosomal DNA was prepared, digested with *Hin*dIII (-2 μg), and electrophoresed through a 0.8% agarose gel. Transfer of DNA from the gel to nitrocellulose filter was performed by standard capillary method. The filter was probed with the PCR products of the *mat1-P* and *mat1-M* (i.e., mixtures of 0.7- and 0.9-kb DNA fragments), and detected with the Alkaphos direct labeling system (Amersham Pharmacia Biotech). PFGE was carried out as following conditions; 0.8% chromosomal grade agarose (BIO-RAD) in 1x TAE at 14°C; electrode angle, 106°; two state mode, 30 min; voltage gradient, 2V/cm; total running time, 48hrs. Upon electrophoretic separation, the gel was allowed to Southern blot analysis probed with the DNA fragments

encoding 18S rRNA.

UV and MMS sensitivity assays

Cells were usually grown to mid-exponential phase in YES media, diluted to appropriate concentrations, plated to a final cell number of 500-1,000 cells, followed by UV irradiation at various doses of exposures (FUNA-UV-Linker, FS 800) and incubated at 30°C for four days. Cell survival was measured by counting the colony numbers as viable cells after incubation. On the other hand, MMS was added to the concentration of 0.1% to mid-logarithmic phase cells suspended in 5 ml of water in a 50 ml plastic tube, and the mixture was incubated at 30°C for the indicated time. Samples were taken from the cultures and mixed with an equal volume of 20% $Na_2S_2O_3$ to inactivate MMS. The cells were then washed with water, re-suspended in 1 ml of water, appropriately diluted, plated onto YES plates, and incubated at 30°C for four days before calculating the cell survival rate.

Ade$^+$ recombination assay

Ade6$^+$ recombination was monitored as follows. Briefly, all the isogenic strains harboring *ade6* heteroallelic duplication derived from the strain PS1 were grown for four days on YES complete medium. The cells from a single colony

were suspended in sterile water and spread at a density of approximately 10^5 cells per plate onto EMM2 medium supplemented with guanine (50 mg/ml) to prevent adenine uptake and select for Ade^+ recombinants. Also, the cells were plated at appropriate dilutions to determine the total cell number on YES. After incubation for four days at 30°C, the number of Ade^+ recombinants and the total cell number were counted. The rates of Ade^+ reversion were calculated according to the median method described by Lea and Coulson (Lea and Coulson, 1949). The ratios of Ade^+Ura^+ to Ade^+Ura^- recombinants were determined by replica-plating total Ade^+ cells onto EMM2 lacking adenine and uracil. Assays were performed in triplicate with at least three independent colonies, and then recombination frequencies were determined and averaged.

Silencing assay

For qualitative colony color assay of repression of the *ade*$^+$ gene, freshly grown cells were spread onto YE plates at 100-200 cells per plate. The plates were incubated at 30°C for four days and photographs were taken after additional one day at 4°C. Also, spot test was performed to evaluate the expression levels of the *ura4*$^+$ gene. *S.pombe* cultures were grown to stationary phase in nonselective medium (N/S). Series of ten-fold dilutions were spotted onto N/S, uracil-free, or counterselective FOA plate, incubated at 30°C for four to six days until full growth was achieved.

Estimation of homothallic conversion frequency

The homothallic conversion frequency was estimated based on the following considerations. Starting from a single h^{+N}*ubc7*$^-$ cell which still has h^{+N}-type of *mat1* structure, the h^{+N} type cell population after X cell divisions is $(1\text{-}p)^{X\text{-}1}$, where conversion from h^{+N} type to h^{90} type cells occurs irreversibly at a frequency of p per cell division. For simplicity, it is assumed that neither type of cell has a growth advantage. Experimentally, the starting h^{+N}*ubc7*$^-$ single cell was a spore from tetrad dissection of $h^{+N/-}$*ubc7*$^{+/-}$ diploid cells (PY34), and the number of cell divisions, X, was calculated from the total number of cells in the colony from which the genomic DNA was prepared for Southern blot analysis. The h^{+N} type cell population was estimated from the amount of h^{+N}-specific DNA fragments (*mat3:1*/8.2-kb and *mat1:3*/6.7-kb *Hin*dIII fragments) detected in the Southern blots probed using *mat* sequences. Conversely, the increase of the h^{90}-type cell population was measured by the appearance of *mat1*/10.4-kb *Hin*dIII fragments. In typical cases, no hybridization signals for DNA fragments specific for the h^{+N}-type cells could be detected after the cells had divided 24-25 times.

ACKNOWLEGEMENTS

I thank Drs. M. Yamamoto, O. Niwa and J. Kohli for the generous gifts of the strains. I specially thank Professor F. Yamao for his faithful supervision and scientific encouragement during my doctoral course. I also acknowledge Professor H. Iwasaki and Y. Akamatsu for enthusiastic discussions and comprehensive suggestions about this thesis. I am very grateful to Professors H. Araki, T. Ikemura, H. Sasaki, T. Kakutani, H. Mitsuzawa, and A. Toh-e for helpful discussions and critical comments. I appreciate Professors N. Shimamoto and T. Takano for statistical assistance. I also thank E. Suzuki for technical assistance. Finally, I'd like to honor my wife and lovely two sons with the degree of Ph.D.

REFERENCES

Alfa, C., Fantes, P., Hyams, J., McLeod, M., and Warbrick, E. (1993). Experiments with fission yeast. A laboratory couerse mannual. CSHL PRESS.

Alleva, J. L., and Doetsch, P. W. (1998). Characterization of *Schizosaccharomyces pombe* Rad2 protein, a FEN-1 homolog. Nucleic Acids Res ***26***, 3645-3650.

Alleva, J. L., and Doetsch, P. W. (2000). The nature of the 5'-terminus is a major determinant for DNA processing by *Schizosaccharomyces pombe* Rad2p, a FEN-1 family nuclease. Nucleic Acids Res ***28***, 2893-2901.

Arcangioli, B. (1998). A site- and strand-specific DNA break confers asymmetric switching potential in fission yeast. Embo J ***17***, 4503-4510.

Arcangioli, B., and de Lahondes, R. (2000). Fission yeast switches mating type by a replication-recombination coupled process. Embo J ***19***, 1389-1396.

Bahler, J., Wu, J. Q., Longtine, M. S., Shah, N. G., McKenzie, A., 3rd, Steever, A. B., Wach, A., Philippsen, P., and Pringle, J. R. (1998). Heterologous modules for efficient and versatile PCR-based gene targeting in *Schizosaccharomyces pombe*. Yeast ***14***, 943-951.

Beach, D., and Klar, A. J. S. (1984a). Rearrangements of the transposable mating-type cassetes of fission yeast. EMBO J ***3***, 603-610.

Beach, D. H., and Klar, A. J. (1984b). Rearrangements of the transposable mating-type cassettes of fission yeast. Embo J ***3***, 603-610.

Chen, P., Johnson, P., Sommer, T., Jentsch, S., and Hochstrasser, M. (1993). Multiple ubiquitin-conjugating enzymes participate in the in vivo degradation of the yeast MAT alpha 2 repressor. Cell ***74***, 357-369.

Choi, E. S., Kim, H. S., Jang, Y. K., Hong, S. H., and Park, S. D. (2002). Two ubiquitin-conjugating enzymes, Rhp6 and UbcX, regulate heterochromatin silencing in *Schizosaccharomyces pombe*. Mol Cell Biol ***22***, 8366-8374.

Dalgaard, J. Z., and Klar, A. J. (1999). Orientation of DNA replication establishes mating-type switching pattern in *S. pombe*. Nature ***400***, 181-184.

Dalgaard, J. Z., and Klar, A. J. (2000). swi1 and swi3 perform imprinting, pausing, and termination of DNA replication in *S. pombe*. Cell ***102***, 745-751.

de Wind, N., Dekker, M., Berns, A., Radman, M., and te Riele, H. (1995). Inactivation of the mouse Msh2 gene results in mismatch repair deficiency, methylation tolerance, hyperrecombination, and predisposition to cancer. Cell ***82***, 321-330.

Deshaies, R. J. (1999). SCF and Cullin/Ring H2-based ubiquitin ligases. Annu Rev Cell Dev Biol ***15***, 435-467.

Fleck, O., Heim, L., and Gutz, H. (1990). A mutated swi4 gene causes duplications in the mating-type region of *Schizosaccharomyces pombe*. Curr Genet ***18***, 501-509.

Friedberg, E. C., Walker, G. C., and Siede, W. (1995). DNA repair and mutagenesis Washington DC, ASM Press.

Grewal, S. I., Bonaduce, M. J., and Klar, A. J. (1998). Histone deacetylase homologs regulate epigenetic inheritance of transcriptional silencing and chromosome segregation in fission yeast. Genetics ***150***, 563-576.

Grewal, S. I., and Elgin, S. C. (2002). Heterochromatin: new possibilities for the inheritance of structure. Curr Opin Genet Dev ***12***, 178-187.

Grossenbacher-Grunder, A. M., and Thuriaux, P. (1981). Spontaneous and UV-induced recombination in radiation-sensitive mutants of *Schizosaccharomyces pombe*. Mutat Res ***81***, 37-48.

Hershko, A., and Ciechanover, A. (1998). The Ubiquitin System. Ann Rev Biochem ***67***, 425-479.

Ho, J. C., Warr, N. J., Shimizu, H., and Watts, F. Z. (2001). SUMO modification of Rad22, the *Schizosaccharomyces pombe* homologue of the recombination protein Rad52. Nucleic Acids Res ***29***, 4179-4186.

Hochstrasser, M. (1996). Ubiquitin-dependent protein degradation. Annu Rev Genet ***30***, 405-439.

Hoege, C., Pfander, B., Moldovan, G. L., Pyrowolakis, G., and Jentsch, S. (2002). RAD6-dependent DNA repair is linked to modification of PCNA by ubiquitin and SUMO. Nature ***419***, 135-141.

Huang, H., Kahana, A., Gottschling, D. E., Prakash, L., and Liebman, S. W. (1997). The ubiquitin-conjugating enzyme Rad6 (Ubc2) is required for silencing in *Saccharomyces cerevisiae*. Mol Cell Biol ***17***, 6693-6699.

Kanaar, R., and Hoeijmakers, J. H. (1997). Recombination and joining: different means to the same ends. Genes Funct ***1***, 165-174.

Kanaar, R., Hoeijmakers, J. H., and van Gent, D. C. (1998). Molecular mechanisms of DNA double strand break repair. Trends Cell Biol ***8***, 483-489.

Kelly, M., Burke, J., Smith, M., Klar, A., and Beach, D. (1988). Four mating-type genes control sexual differentiation in the fission yeast. Embo J *7*, 1537-1547.

Klar, A. J., and Miglio, L. M. (1986). Initiation of meiotic recombination by double-strand DNA breaks in *S. pombe*. Cell ***46***, 725-731.

Kobayashi, T., Heck, D. J., Nomura, M., and Horiuchi, T. (1998). Expansion and contraction of ribosomal DNA repeats in *Saccharomyces cerevisiae*: requirement of replication fork blocking (Fob1) protein and the role of RNA polymerase I. Genes Dev

12, 3821-3830.

Kobayashi, T., and Horiuchi, T. (1996). A yeast gene product, Fob1 protein, required for both replication fork blocking and recombinational hotspot activities. Genes Cells *1*, 465-474.

Kominami, K., Ochotorena, I., and Toda, T. (1998). Two F-box/WD-repeat proteins Pop1 and Pop2 form hetero- and homo-complexes together with cullin-1 in the fission yeast SCF (Skp1-Cullin-1-F-box) ubiquitin ligase. Genes Cells *3*, 721-735.

Kovalenko, O. V., Plug, A. W., Haaf, T., Gonda, D. K., Ashley, T., Ward, D. C., Radding, C. M., and Golub, E. I. (1996). Mammalian ubiquitin-conjugating enzyme Ubc9 interacts with Rad51 recombination protein and localizes in synaptonemal complexes. Proc Natl Acad Sci U S A *93*, 2958-2963.

Lea, D. E., and Coulson, C. A. (1949). The distribution of the number of mutants in bacterial populations. J Genet *49*, 264-285.

Maleszka, R., and Clark-Walker, G. D. (1993). Yeasts have a four-fold variation in ribosomal DNA copy number. Yeast *9*, 53-58.

Mizukami, T., Chang, W. I., Garkavtsev, I., Kaplan, N., Lombardi, D., Matsumoto, T., Niwa, O., Kounosu, A., Yanagida, M., Marr, T. G., and et al. (1993). A 13 kb resolution cosmid map of the 14 Mb fission yeast genome by nonrandom sequence-tagged site mapping. Cell *73*, 121-132.

Moreno, S., Klar, A., and Nurse, P. (1991). Methods in Enzymology, Academic Press

Mundt, K. E., Liu, C., and Carr, A. M. (2002). Deletion mutants in COP9/signalosome subunits in fission yeast *Schizosaccharomyces pombe* display distinct phenotypes. Mol Biol Cell *13*, 493-502.

Murray, J. M., Tavassoli, M., al-Harithy, R., Sheldrick, K. S., Lehmann, A. R., Carr, A.

M., and Watts, F. Z. (1994). Structural and functional conservation of the human homolog of the *Schizosaccharomyces pombe* rad2 gene, which is required for chromosome segregation and recovery from DNA damage. Mol Cell Biol ***14***, 4878-4888.

Nasim, A., Young, P., and Johnson, B. F. (1989). Molecular biology of the fission yeast, Academic Press.

Nielsen, I. S., Nielsen, O., Murray, J. M., and Thon, G. (2002). The fission yeast ubiquitin-conjugating enzymes UbcP3, Ubc15, and Rhp6 affect transcriptional silencing of the mating-type region. Eukaryot Cell ***1***, 613-625.

Nielsen, O., and Egel, R. (1989). Mapping the double-strand breaks at the mating-type locus in fission yeast by genomic sequencing. Embo J ***8***, 269-276.

Ohta, T., Michel, J. J., Schottelius, A. J., and Xiong, Y. (1999). ROC1, a homolog of APC11, represents a family of cullin partners with an associated ubiquitin ligase activity. Mol Cell ***3***, 535-541.

Ohta, T., and Xiong, Y. (2001). Phosphorylation- and Skp1-independent in vitro ubiquitination of E2F1 by multiple ROC-cullin ligases. Cancer Res ***61***, 1347-1353.

Osaka, F., Seino, H., Seno, T., and Yamao, F. (1997). A ubiquitin-conjugating enzyme in fission yeast that is essential for the onset of anaphase in mitosis. Mol Cell Biol ***17***, 3388-3397.

Osman, F., Adriance, M., and McCready, S. (2000). The genetic control of spontaneous and UV-induced mitotic intrachromosomal recombination in the fission yeast Schizosaccharomyces pombe. Curr Genet ***38***, 113-125.

Paques, F., and Haber, J. E. (1999). Multiple pathways of recombination induced by double-strand breaks in Saccharomyces cerevisiae. Microbiol Mol Biol Rev ***63***, 349-404.

Pickart, C. M. (2001). Ubiquitin enters the new millennium. Mol Cell ***8***, 499-504.

Rayssiguier, C., Thaler, D. S., and Radman, M. (1989). The barrier to recombination between *Escherichia coli* and *Salmonella typhimurium* is disrupted in mismatch-repair mutants. Nature ***342***, 396-401.

Schuchert, P., and Kohli, J. (1988). The ade6-M26 mutation of *Schizosaccharomyces pombe* increases the frequencyof crossing over. Genetics ***119***, 507-515.

Shinohara, A., Ogawa, H., and Ogawa, T. (1992). Rad51 protein involved in repair and recombination in *S. cerevisiae* is a RecA-like protein. Cell ***69***, 457-470.

Singh, J., Goel, V., and Klar, A. J. (1998). A novel function of the DNA repair gene rhp6 in mating-type silencing by chromatin remodeling in fission yeast. Mol Cell Biol ***18***, 5511-5522.

Sommer, T., and Wolf, D. H. (1997). Endoplasmic reticulum degradation: reverse protein flow of no return. Faseb J ***11***, 1227-1233.

Stewart, E., Chapman, C. R., Al-Khodairy, F., Carr, A. M., and Enoch, T. (1997). rqh1+, a fission yeast gene related to the Bloom's and Werner's syndrome genes, is required for reversible S phase arrest. Embo J ***16***, 2682-2692.

Styrkarsdottir, U., Egel, R., and Nielsen, O. (1993). The smt-0 mutation which abolishes mating-type switching in fission yeast is a deletion. Curr Genet ***23***, 184-186.

Szankasi, P., Heyer, W. D., Schuchert, P., and Kohli, J. (1988). DNA sequence analysis of the ade6 gene of *Schizosaccharomyces pombe*. Wild-type and mutant alleles including the recombination host spot allele ade6-M26. J Mol Biol ***204***, 917-925.

Wood, V., Gwilliam, R., Rajandream, M. A., Lyne, M., Lyne, R., Stewart, A., Sgouros, J., Peat, N., Hayles, J., Baker, S., *et al.* (2002). The genome sequence of *Schizosaccharomyces pombe*. Nature ***415***, 871-880.

Worth, L., Jr., Clark, S., Radman, M., and Modrich, P. (1994). Mismatch repair proteins MutS and MutL inhibit RecA-catalyzed strand transfer between diverged DNAs. Proc Natl Acad Sci U S A ***91***, 3238-3241.

Yamao, F. (1999). Ubiquitin system: selectivity and timing of protein destruction. J Biochem (Tokyo) ***125***, 223-229.

Young, J. A., Schreckhise, R. W., Steiner, W. W., and Smith, G. R. (2002). Meiotic recombination remote from prominent DNA break sites in *S. pombe*. Mol Cell ***9***, 253-263.

Zhou, C., Seibert, V., Geyer, R., Rhee, E., Lyapina, S., Cope, G., Deshaies, R. J., and Wolf, D. A. (2001). The fission yeast COP9/signalosome is involved in cullin modification by ubiquitin-related Ned8p. BMC Biochem ***2:7***.

Table 1. *S.pombe* strains constructed and used in this study

Strain	Genotype	Source
JY741	*h⁻ leu1-32 ura4-D18 ade6-M216*	M.Yamamoto
JY746	*h^{+N} leu1-32 ura4-D18 ade6-M210*	M.Yamamoto
JY878	*h^{90} leu1-32 ura4-D18 ade6-M216*	M.Yamamoto
Z436	*h^{+S} leu1-32 ura4-D18*	O.Niwa
PY119	*h⁻ smt-0 leu1-32 ura4-D18 his3-D1 arg3-D1*	O.Nielson
PY62	*h^{+N} smt-0 leu1-32 ura4-D18 his3-D1 arg3-D1*	This study
PY31	*h⁻ leu1-32 ura4-D18 ade6-M216 $ubc7^{+}$::$ura4^{+}$*	This study
PY32[a]	*h^{+N} leu1-32 ura4-D18 ade6-M216 $ubc7^{+}$::$ura4^{+}$*	This study
PY34	*h⁻/h^{+N} leu1-32/leu1-32 ura4-D18/ura4-D18 $ubc7^{+}$/$ubc7^{+}$::$ura4^{+}$*	This study
PY45	*h^{90} leu1-32 ura4-D18 ade6-M216 $ubc7^{+}$::$ura4^{+}$*	This study
PY46	*h^{+S} leu1-32 ura4-D18 $ubc7^{+}$::$ura4^{r}$*	This study
PY55	*h^{+S} leu1-32 ura4-D18 ade6-M26/int::pUC8/$ura4^{+}$/ade6-L469*	J.Kohli
PYK62	*h^{+S} leu1-32 ura4-D18 ade6-M26/int::pUC8/$ura4^{+}$/ade6-L469$ubc7^{+}$::$G418^{r}$*	This study
PY74	*h^{+S} leu1-32 ura4-D18 ade6-M26/int::pUC8/$ura4^{+}$/ade6-L469$rad2^{+}$::$LEU2^{+}$*	This study
PY76	*h^{+S} leu1-32 ura4-D18 ade6-M26/int::pUC8/$ura4^{+}$/ade6-L469$rad2^{+}$::$LEU2^{+}$$ubc7^{+}$::$G418^{r}$*	This study
PY64	*h⁻ smt-0 leu1-32 ura4-D18 his3-D1 arg3-D1 $rhp51^{+}$::$ura4^{+}$*	This study

PYK46	*h⁻ leu1-32 ura4-D18 ade6-M216 ubc7⁺::G418ʳ*	This study
PYK57	*h⁻ smt-0 leu1-32 ura4-D18 his3-D1 arg3-D1 ubc7⁺::G418ʳ*	This study
PYK60	*h⁻ smt-0 leu1-32 ura4-D18 his3-D1 arg3-D1 rhp51⁺::ura4⁺ ubc7⁺::G418ʳ*	This study
PYK61	*h⁺ᴺ smt-0 leu1-32 ura4-D18 his3-D1 arg3-D1 ubc7⁺::G418ʳ*	This study
PY52	*h⁺ˢ leu1-32 ura4-D18 pcu3⁺::ura4⁺*	This study
FY340	*TM1(NcoI)-ura4 Random int. h⁺ leu1-32 ade6-210 ura4-DS/E*	R.C.Allshire
PYK44	*TM1(NcoI)-ura4 Random int. h⁺ leu1-32 ade6-210 ura4-DS/E ubc7⁺::G418ʳ*	This study
FY1193	*h⁺ ade6-210 leu1-32 ura4-D18 imr1L(NcoI)::ura4⁺otr1R(SphI)::ade6⁺*	R.C.Allshire
PYK52	*h⁺ ade6-210 leu1-32 ura4-D18 imr1L(NcoI)::ura4⁺otr1R(SphI)::ade6⁺ubc7::G418ʳ*	This study

Table 2. UV-induced intrachromosomal recombination between *ubc7*$^{+}$ and *ubc7*$^{-}$ cells.

	ubc7^{+}		*ubc7*$^{-}$	
UV (J/m^2)	0	100	0	100
Ade^{+} *recombination*				
Rate (x10^{-4})[a]	0.9	3.3	1.1	5.0
Relative increase[b]	1.0	3.7	1.0	4.7
Product ratio in %				
Ade^{+}Ura^{+}	33	60	37	74
Ade^{+}Ura^{-}	67	40	63	26

[a] Reversion rate was calculated from the mean of the means of two independent assays.

[b] Increase in recombination rate relative to the unirradiated control.

[C] The ratio of Ade^{+}Ura^{+} or Ade^{+}Ura^{-} to total Ade^{+} recombinants was determined in percentage.

Table 3. Drastic increase in the intrachromosomal recombination caused by the concurrent *rad2* mutation.

	Ade$^+$ recombination		*Product ratio in %*[d]	
Strain[a]	Rate (x10^{-4})[b]	Relative increase[c]	Ade$^+$Ura$^-$	Ade$^+$Ura$^+$
wild –type	1.11	1.00	50 (1.0)	50 (1.0)
ubc7$^-$rad2$^+$	1.35	1.20	50 (1.2)	50 (1.2)
ubc7$^+$rad2$^-$	4.10	3.70	75 (5.5)	25 (1.8)
ubc7$^-$rad2$^-$	12.2	11.0	70 (15.4)	30 (6.6)

[a] All the strains are isogenic to *h^{+s} leu1-32 ura4-D18 ade6-M26int::pUC8/ura4$^+$/ade6-L469*.

[b] Reversion rate was calculated from three independent assays according to the median method.

[c] Increase in recombination rate relative to the wild-type strain.

[d] Values in parentheses indicate the increase of the calculated recombination rate relative to that of the wild-type strain.

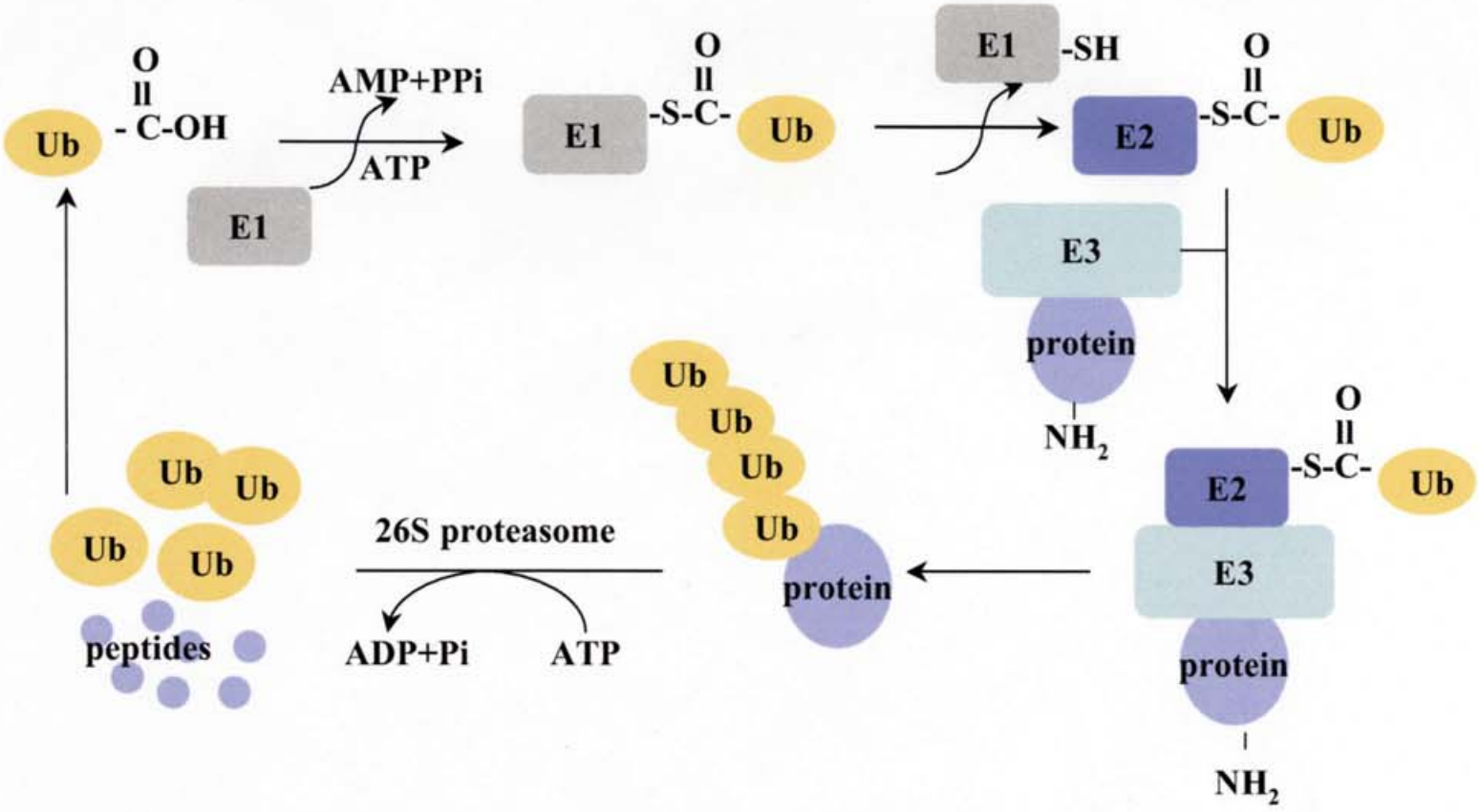

Fig. 1. The ubiquitin pathway. Free ubiquitin is activated in an ATP-dependent manner with the formation of a thiol ester linkage between E1 and carboxyl terminus of ubiquitin. Ubiquitin is transferred to one of a number of different E2s. E2 associates with E3s, which might or might not have protein already bound. The polyubiquitinated protein is then targeted for degradation by 26S proteasome. Ub, ubiquitin; E1, ubiquitin-activating ezyme; E2, ubiquitin-conjugating enzyme; E3, ubiquitin ligase.

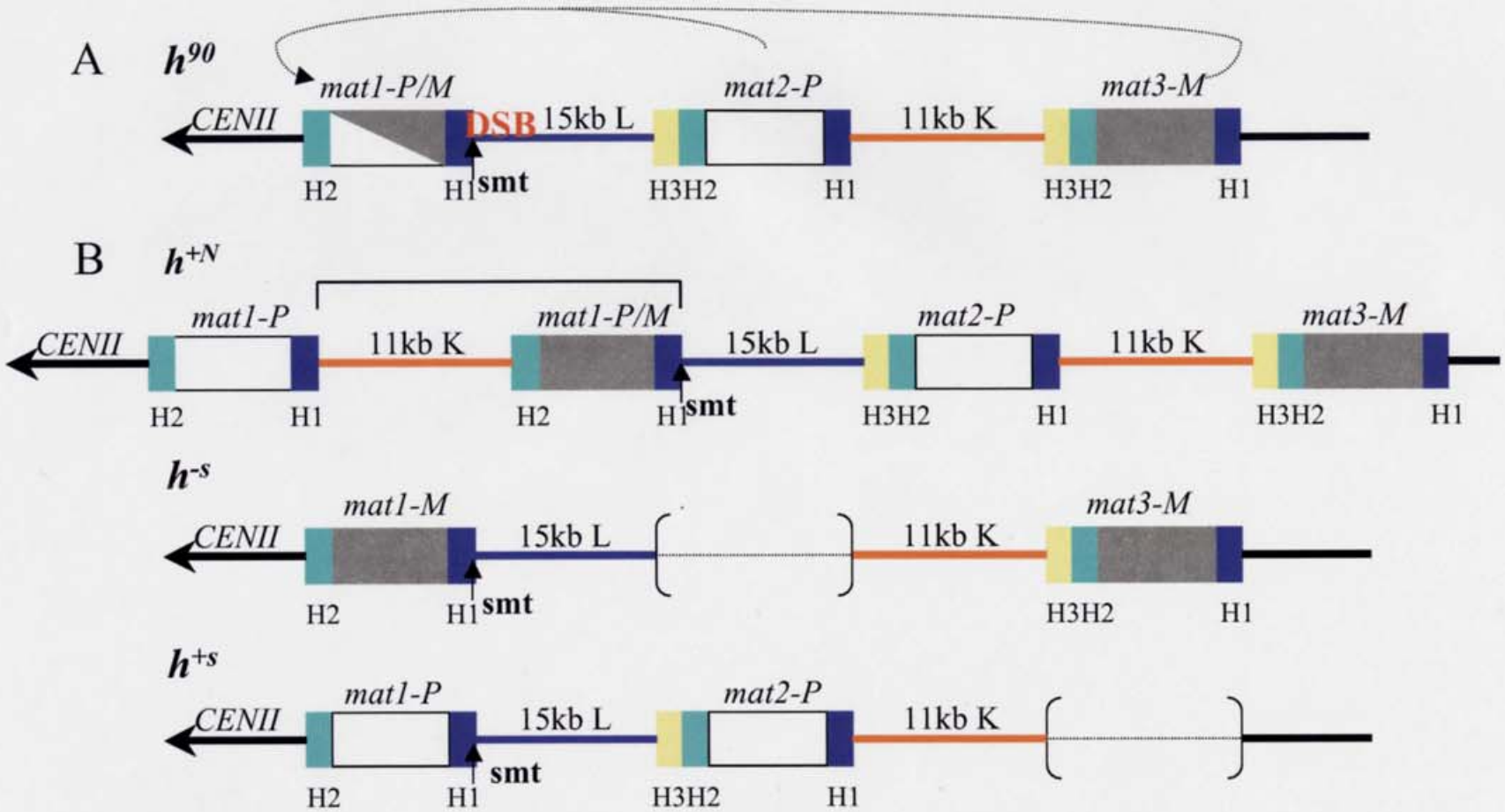

Fig. 2. Physical map of mating-type cassettes in *S.pombe*. (A) In homothallic h^{90} cell, the *mat1* locus contains the *P* or *M* allele, which is copied from *mat2-P* or *mat3-M*, as indicated by dot lines. The H1 and H2 homology sequences are common to all cassettes, whereas the H3 is common to only the silent *mat2-P* and *mat3-M* loci. The intervening sequences between cassettes are L (blue lines) and K (orange lines) regions, respectively. The *smt* (black arrows) is required to initiate DSB formation and subsequent mating-type switching. (B) Illustration of several types of heterothallic configurations. h^{-s} and h^{+s} types, which the opposite cassette is deleted, respectively, as indicated by parenthesis. Note that the heterothallic h^{+N} configuration has two tandem segments at *matl* locus. The active *P* allele is located at *mat1:2* and determines the mating-type, while a silent *M* allele is located in the *mat3:1* cassette.

A

```
SpUbc7          MSKAMALRRLMKEYKELTENGPDGITAGPSNEDDFFTWDCLIQGPDGTPFEGGLYPATLK
HsUbcH7         -MAGTALKRLMAEYKQLTLNPPEGIVAGPMNEENFFEWEALIMGPEDTCFEFGVFPAILS
ScUbc7          -MSKTAQKRLLKELQQLIKDSPPGIVAGPKSENNIFIWDCLIQGPPDTPYADGVFNAKLE
                     * :**: * ::*  : * **.*** .*:::* *:.** ** .* :  *:: * *.
SpUbc7          FPSDYPLGPPTLKFECEFFHPNVYKDGTVCISILHAPGDDPNMYESSSERWSPVQSVEKI
HsUbcH7         FPLDYPLSPPKMRFTCEMFHPNIYPDGRVCISILHAPGDDPMGYESSAERWSPVQSVEKI
ScUbc7          FPKDYPLSPPKLTFTPSILHPNIYPNGEVCISILHSPGDDPNMYELAEERWSPVQSVEKI
                ** ****.**.: *  .::***:* :* *******:*****  ** : ************
SpUbc7          LLSVMSMLAEPNDESGANIDACKMWREDREEYCRVVRRLARKTLGL
HsUbcH7         LLSVVSMLAEPNDESGANVDASKMWRDDREQFYKIAKQIVQKSLGL
ScUbc7          LLSVMSMLSEPNIESGANIDACILWRDNRPEFERQVKLSILKSLGF
                ****:***:*** *****:**. :**::* :: : .:    *:**:
```

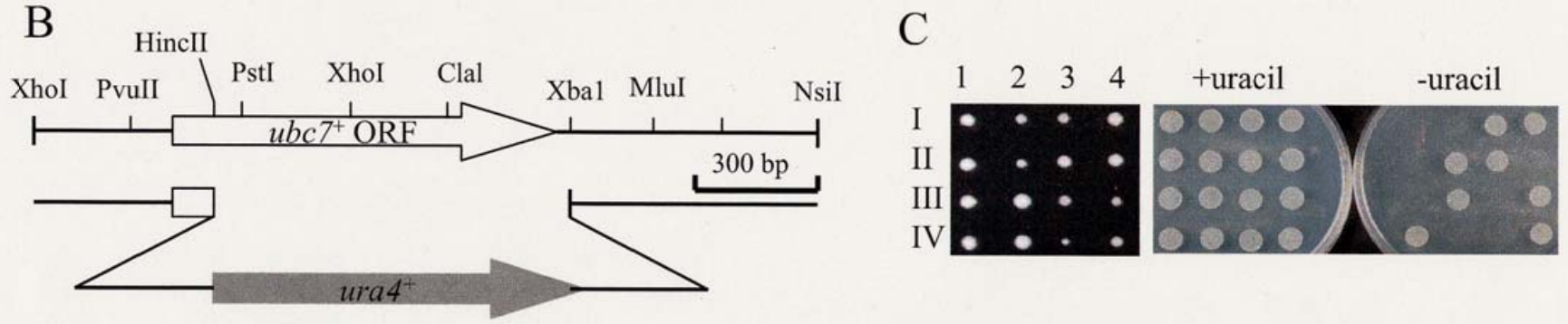

Fig. 3. The *ubc7*$^+$ gene is not essential for cell viability. (A) Alignment of amino acid among *S.cerevisiae* Ubc7, *S.pombe* Ubc7, and *H.sapiens* UbcH7. Asterisks indicate the identical residues. The active site cysteine is marked in red. Accession; *Sc*Ubc7, CAA89125; *Sp*Ubc7, SPBP16F5.04; *Hs*UbcH7, BAA11410. (B) A restriction map of the *ubc7*$^+$ gene. The white arrow indicates the direction and extent of the *ubc7*$^+$ ORF. The *Hinc*II-*Xba*I region of the *ubc7*$^+$ was replaced with a 1.8-kb *ura4*$^+$ gene cassette (gray arrow) for generating an *ubc7*-knockout. (C) Tetrad dissection of the heterozygous diploid for *ubc7* (PY34) is shown. All asci (I-IV) produced four viable spores, which uracil marker exactly segregated 2:2.

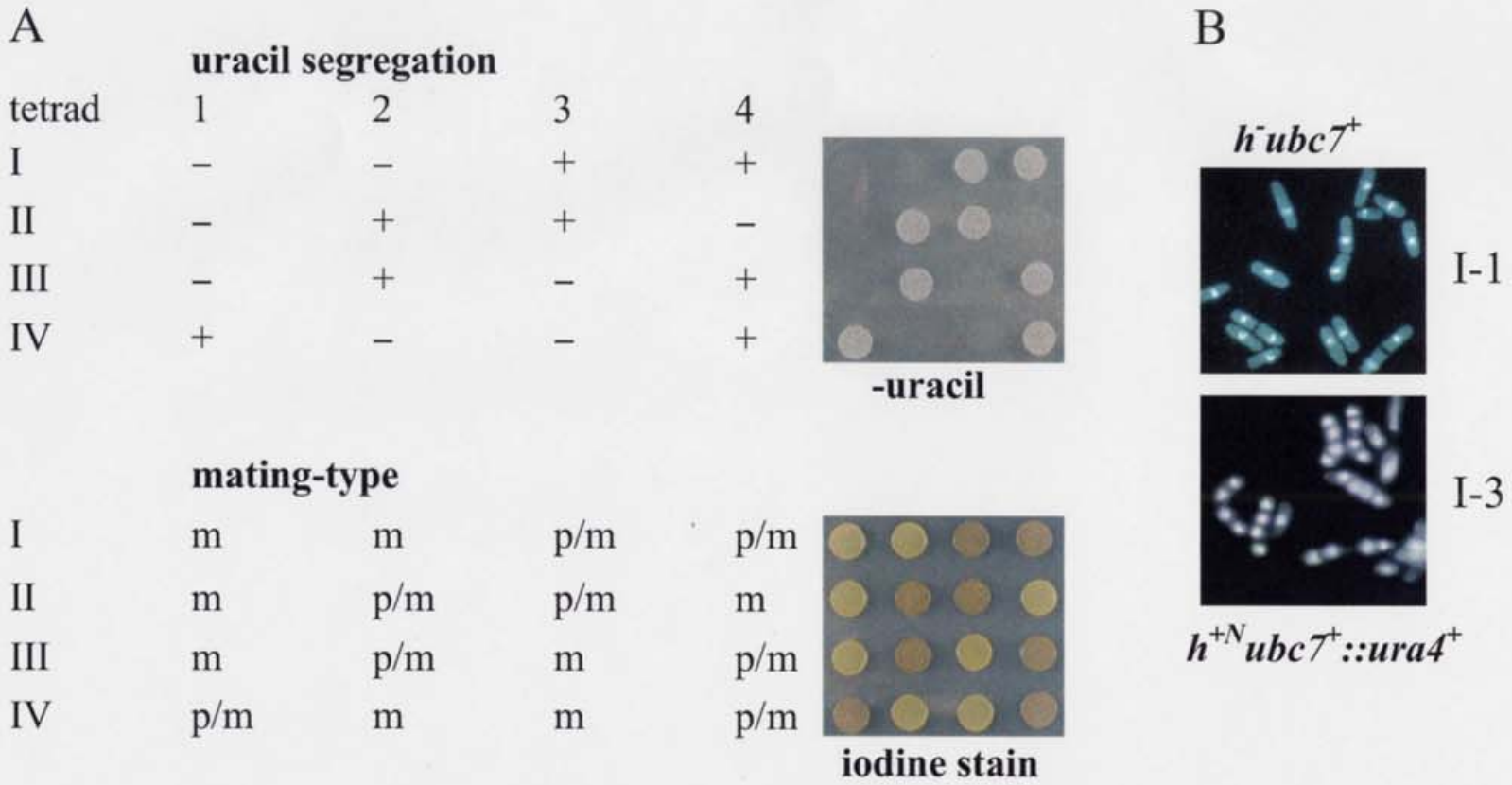

Fig. 4. Ubc7-deficiency stimulates homothallic conversion. (A) The four asci (I-IV) produced four viable spores from tetrad dissection. Upper panel indicates the profile of uracil auxotrophy (-) and prototrophy (+). The mating-type of germinated cells determined by PCR are also shown in lower panel. p, m and p/m indicate plus (P), minus (M) and a mixture of plus and minus (P/M) of the mating-type. p/m and m segregate 2:2, indicating that the p/m phenotype was originated from h^{+N} cells. Uracil prototrophy was also tightly linked with the p/m phenotype, indicating that *ubc7*$^+$ gene was strongly linked to *mat1*. Cells germinated from spores were exposed to iodine vapor: the p/m phenotype was correlated with iodine-positive phenotype (brown color; right side in lower panel). (B) Microscopic features; m (I-1) cells were characterized by vegetative growth of haploid cells and p/m (I-3) cells were characterized by accumulation of zygotes or asci.

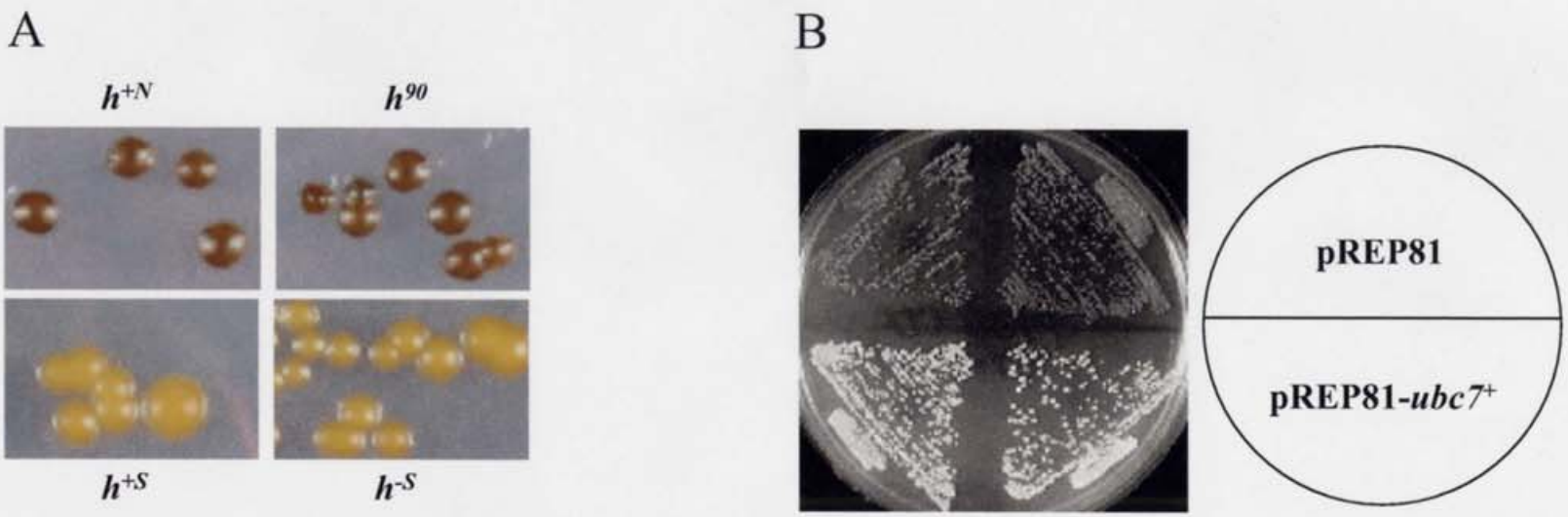

h^{+N} *mat1:2*-P == K == *mat3:1*-M,P -- L -- *mat2:2*-P == K == *mat3:3*-M
h^{90} *mat1*-M,P -- L -- *mat2*-P == K == *mat3-M*
h^{+s} *mat1:1*-P -- L -- *mat2:3*-P
h^{-s} *mat1:1*-M -- L -- *mat2:3*-M

Fig. 5. Ubc7 is required for the maintenance of heterothallism of h^{+N} strain. (A) Direct disruption of the *ubc7*$^{+}$ gene in several types of haploid strains. Each knock-out strain was grown on EMM2 minimal medium and exposed to iodine vapor. h^{90} homothallic strain was used as a positive homothallic control. Note that only h^{+N}*ubc7*$^{-}$ strain was positively stained with iodine. Their *mat* configurations were also shown. (B) The homothallic conversion is an authentic phenotype resulted from Ubc7-defect. Plasmid thiamine-repressible pREP81-*ubc7*$^{+}$ or empty vector pREP81 was introduced to the heterozygous diploid strain (PY34). After tetrad dissection of the resulting recombinant strains, stable Ura^{+} Leu^{+} cells were selected, grown on EMM2 medium and analyzed by iodine staining. The h^{+N}*ubc7*$^{-}$ cells carrying pREP81-*ubc7*$^{+}$ were not stained with iodine, while the cells carrying empty vector gave the positive reaction.

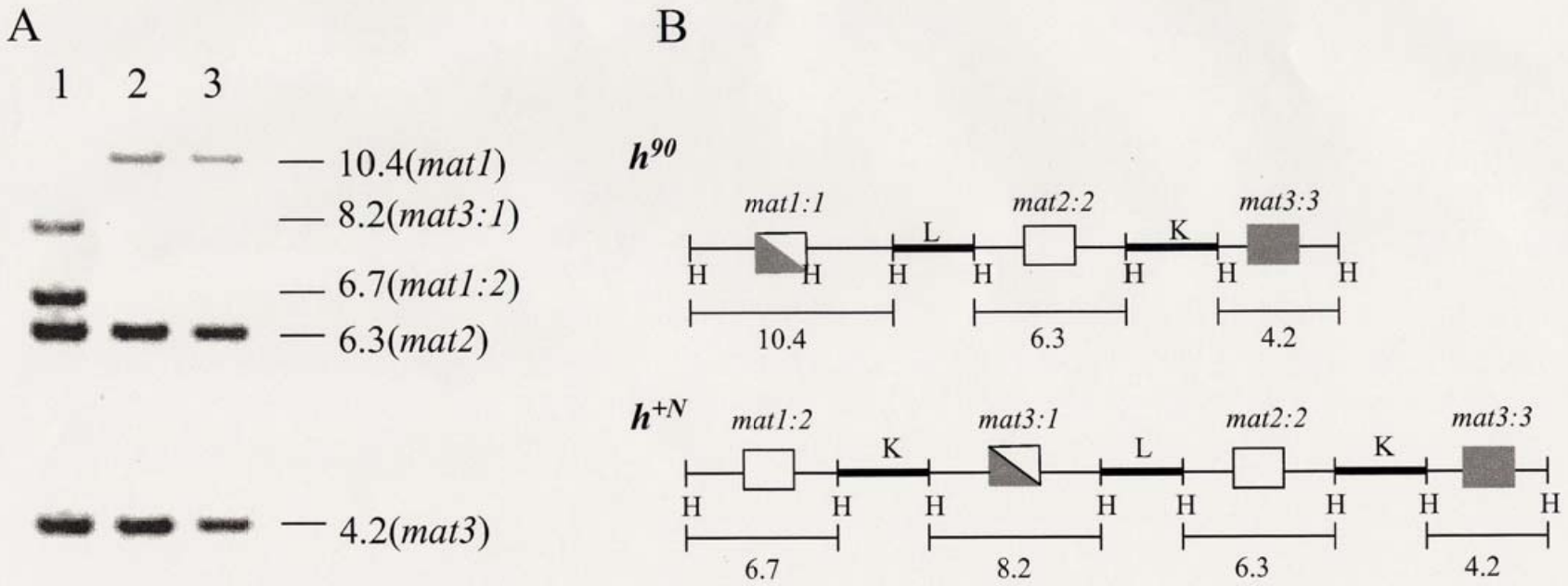

Fig. 6. Ubc7-deficiency induces DNA rearrangement at *mat1* locus. (A) Cells were grown to stationary phase in YES medium and chromosomal DNA was prepared, digested with *Hin*dIII and subjected to Southern analysis. The PCR-amplified DNA fragments of *mat1:1* was used as probe sequences. The sizes of the *Hin*dIII fragments (in kb) and the corresponding cassettes are shown on the right side. Lane 1, $h^{+N}ubc7^{+}$ (JY746); lane 2, $h^{+N}ubc7^{-}$ (PY32); lane 3, $h^{90}ubc7^{+}$ (JY878). (B) Physical arrangement of *mat* cassettes in h^{90} and h^{+N} strains. According to the nomenclature, the *first number* indicates the origin of the proximal flanking sequence, the *second number* the origin of the distal flanking sequence. For example, a *mat3:1* cassette is flanked proximally by K and distally by L, respectively. The *Hin*dIII fragments (in kb) are shown below the cassettes.

A

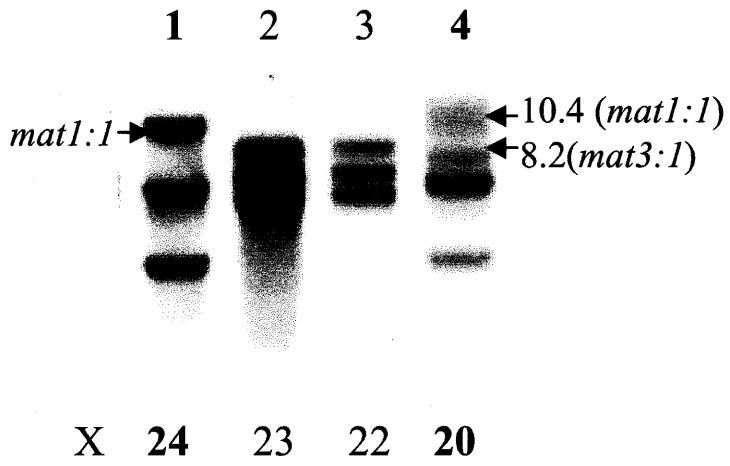

B

Conversion frequency (p)	h^{+N} population
10^{-5}	99.98 %
10^{-4}	99.80 %
10^{-3}	97.60 %
10^{-2}	78.50 %
10^{-1}	8.80 %

Fig. 7. The frequency of homothallic conversion was estimated by measuring the loss of h^{+N}-specific DNA fragments (*mat3:1*/8.2-kb) or the appearance of h^{90}-specific DNA fragments (*mat1:1*/10.4-kb), as described in *Materials and Methods.* (A) Southern blot analysis of genomic *Hin*dIII digests was preformed as shown in Fig. 6A. Four spores from tetrad dissection of $h^{+N/-}ubc7^{+/-}$ diploid cells (PY34) were used as starting cells. After the number of cell divisions, X, was calculated from the total number of cells from which the genomic DNA was prepared. h^{+N}-specific DNA fragments were not detected after the cells had divided 24 times (compare the *mat3:1*/8.2-kb fragment in lanes 1 and 4). Lanes 1 and 4; $h^{+N}ubc7^{-}$, lanes 2 and 3; $h^{-}ubc7^{+}$. (B) The results of simulation are also shown. The rate of homothallic conversion in $h^{+N}ubc7^{-}$ cells was calculated to be on the order of 10^{-1}. See more details in text.

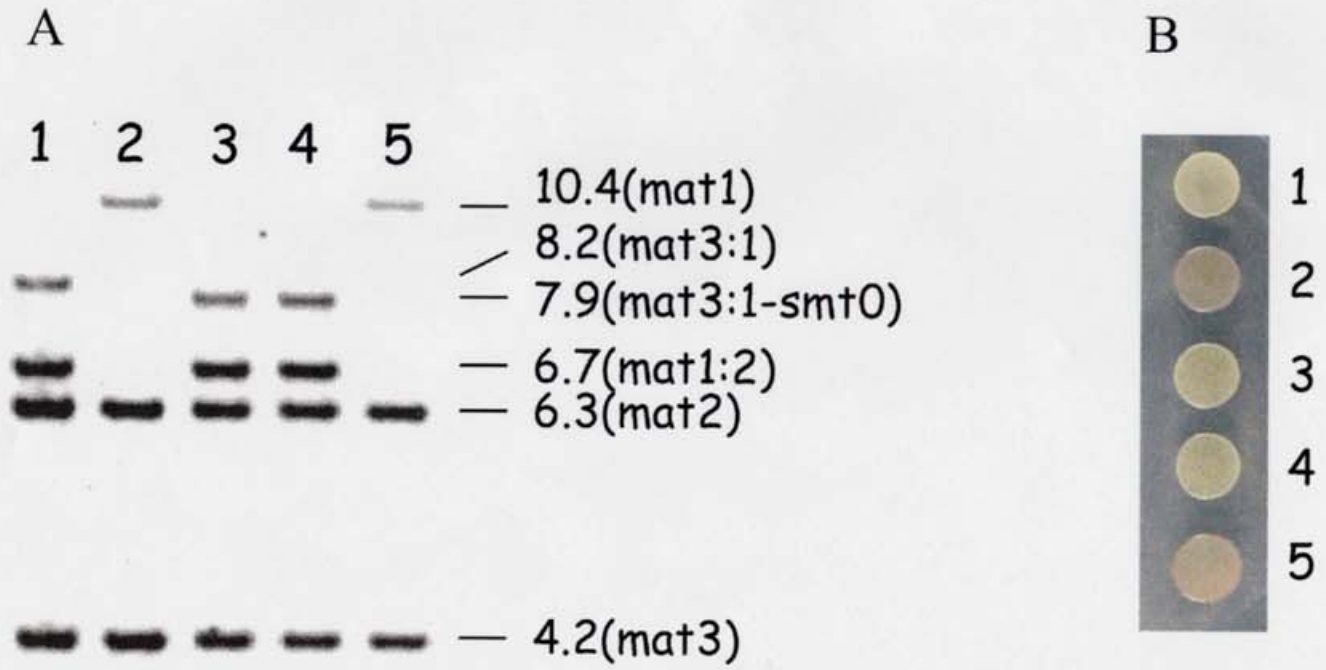

Fig. 8. The *smt* deletion induces neither DNA rearrangement at *mat1* nor homothallic conversion. (A) Southern blot analysis of genomic *Hin*dIII digests was performed as described in Fig. 6A. The *mat3:1* fragment in *smt-0* (7.9-kb; lanes 3 and 4) became shorter compared to the *mat3:1* fragment in smt^+ (8.2-kb; lane 1). The sizes of the *Hin*dIII fragments and the corresponding cassettes are shown on the right side. (B) All the strains shown in A were grown on EMM2 plate, and exposed to iodine vapor. h^{+N}*smt-0ubc7*$^-$ was not stained with iodine, even though the Ubc7 was inactivated (lanes 3 and 4; smt^+ control, lane 2). Lane 1, h^{+N} *ubc7*$^+$ (JY746); lane 2, h^{+N} *ubc7*$^-$ (PY32); lane 3, h^{+N} *smt-0 ubc7*$^+$ (PY119); lane 4, h^{+N} *smt-0 ubc7*$^-$ (PYK61); lane 5, h^{90} *ubc7*$^+$ (JY878).

A

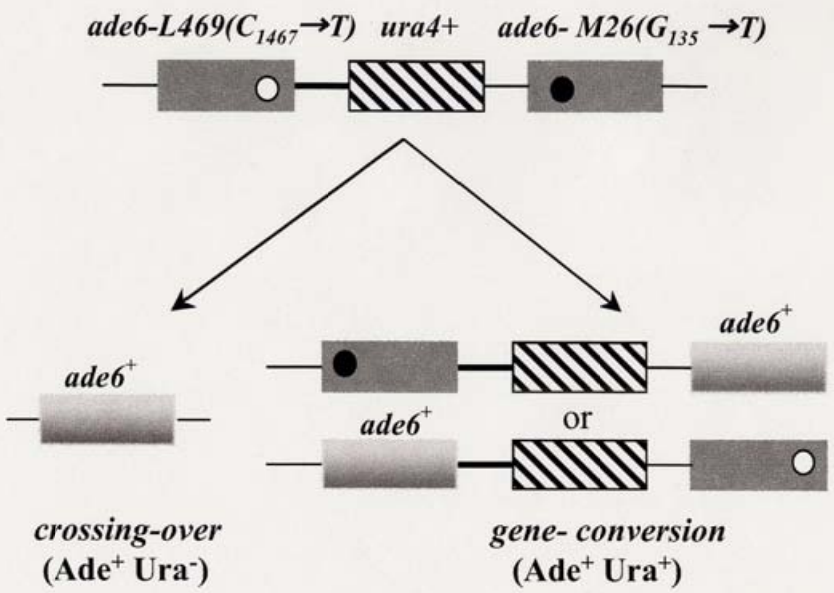

B

	Strains	
	ubc7^{+}	*ubc7*$^{-}$
Ade^{+} *recombination*		
Reversion rate (x10^{-4})	0.9	1.1
Relative increase	1.0	1.2
Product ratio in %		
Ade^{+}Ura^{+}	42	47
Ade^{+}Ura^{-}	58	53

Fig. 9. Ubc7-defect itself has no influence on the intrachromosomal recombination at *ade6* duplication. (A) Schematic drawing of the intrachromosomal recombination substrate and two classes of Ade^{+} recombinants. The light gray boxes correspond to the *ade6*$^{+}$ coding regions. Both black and white circles represent the *ade6-M26* and *ade6-L469* point mutations. (B) Spontaneous intrachromosomal recombination frequencies for *ubc7*$^{+}$ (PY55) and *ubc7*$^{-}$ cells (PYK62). Ade^{+} reversion rate per cell division were determined according to the median method described by Lea and Coulson. The ratio of Ade^{+}Ura^{+} or Ade^{+}Ura^{-} was calculated in percent relative to total Ade^{+} recombinants.

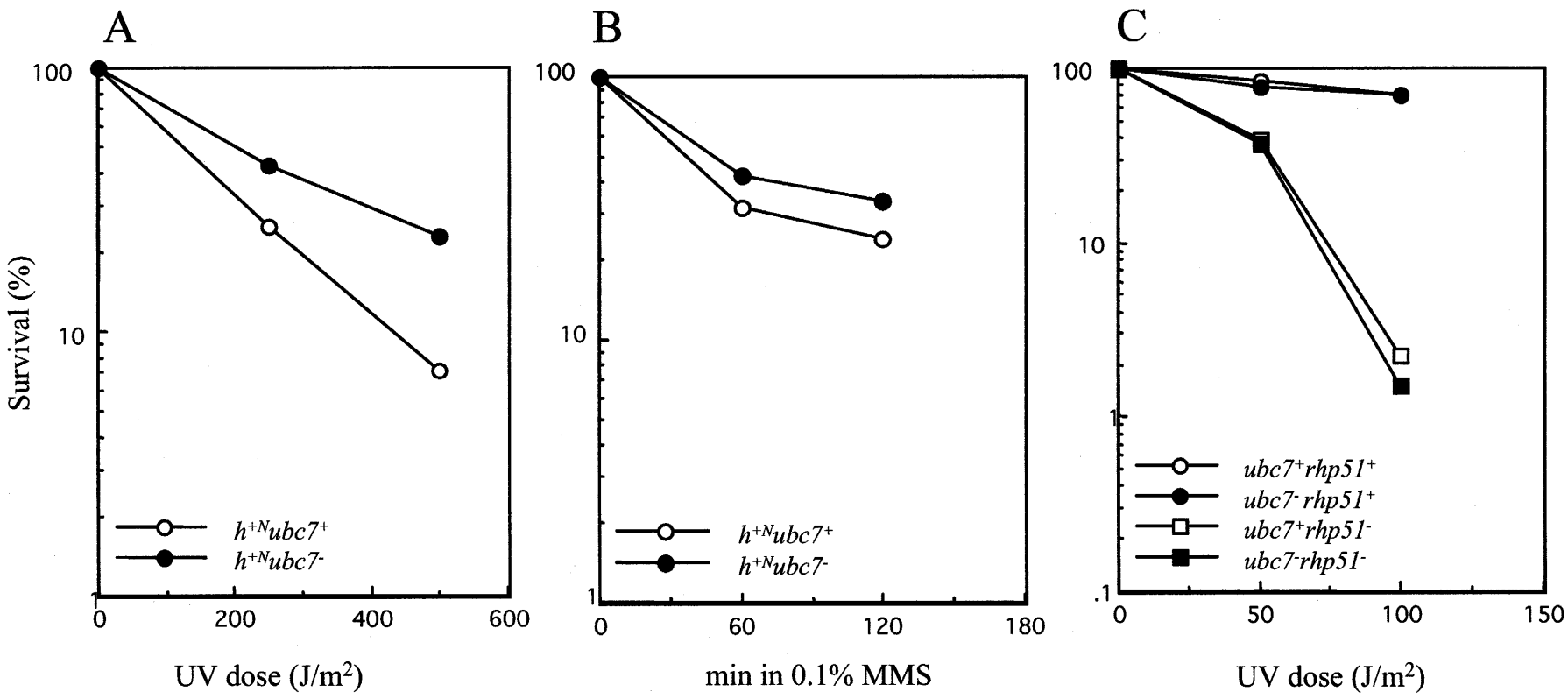

Fig. 10. Ubc7-deficiency causes Rhp51-dependent hyper-resistance to DNA damage. (A) UV sensitivity was measured as described in *Materials and Methods*. $h^{+N}ubc7^{-}$ cells (PY32;closed circles) are hyper-resistant compared to wild -type $h^{+N}ubc7^{+}$ cells (JY746;open circles). (B) MMS killing assay was performed in a liquid culture containing 0.1% MMS. $h^{+N}ubc7^{-}$ cells (PY32; closed circles) were substantially more resistant than $h^{+N}ubc7^{+}$ cells (JY746;open circles). (C) The increased repair activity depending on the function of Rhp51. $h^{-}smt\text{-}0rhp51^{+}$ (PY119;open circles), $h^{-}smt\text{-}0ubc7^{-}$ (PYK57;closed circles), $h^{-}smt\text{-}0rhp51^{-}$ (PY64;open squares), and $h^{-}smt\text{-}0ubc7^{-}rhp51^{-}$ (PYK60;closed squares) were prepared and treated as in A. The results are an average of two independent experiments.

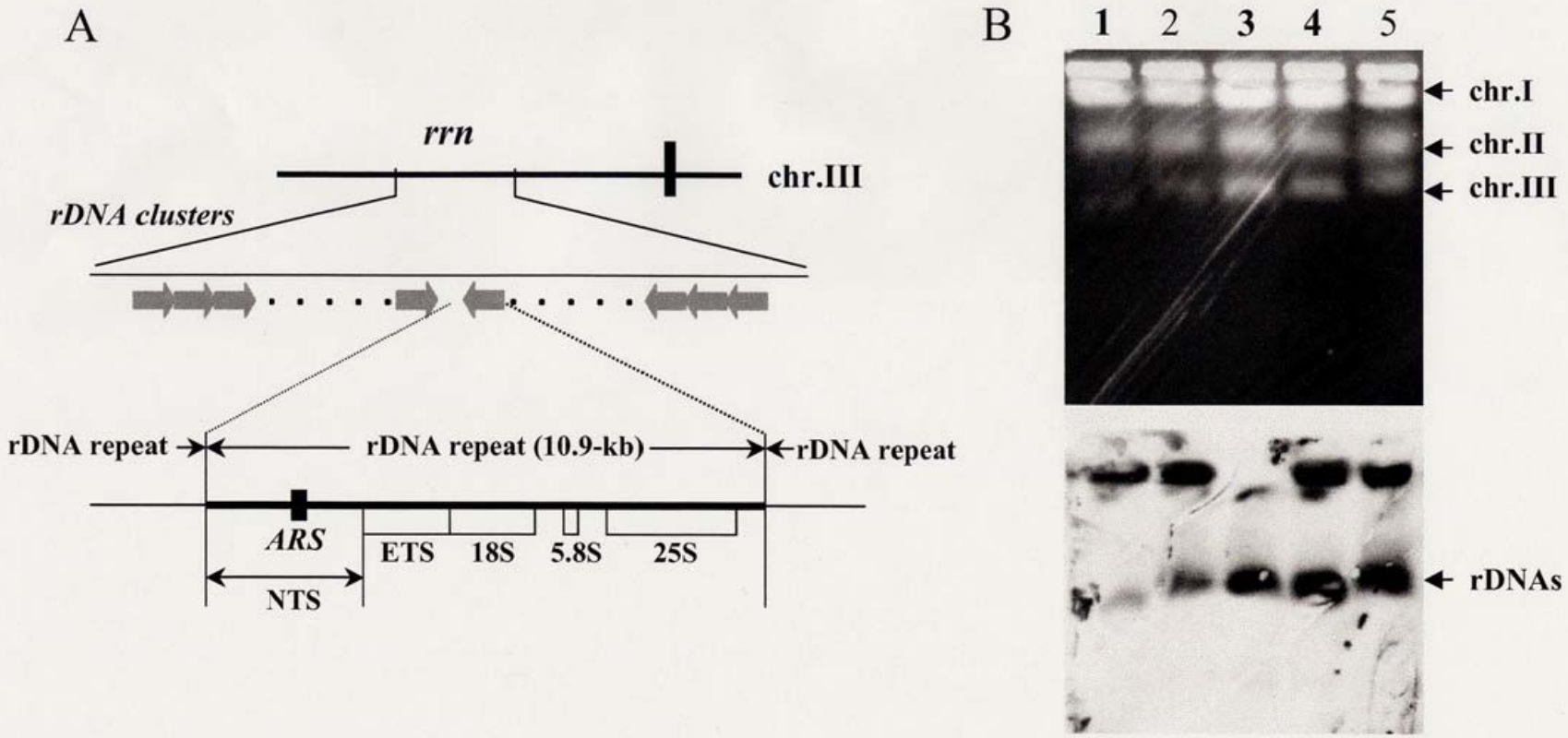

Fig. 11. Ubc7-deficiency enhances recombination at rDNA repeats. (A) Structure of rDNA repeats in *S.pombe.* Location of the ETS (external transcribed spacer;7.9-kb), NTS (nontranscribed spacer;3.0-kb), and ARS (replication origin) are shown. (B) PFGE separation of the chromosomes of the *ubc7* mutant. PFGE was performed as described in *Materials and Methods.* Upper panel ; The ethidium bromide-stained gel of the intact chromosome before Southern analysis. The location of individual chromosome was marked by black arrow. Lower panel ; Southern blot analysis probed with the PCR-amplified DNA fragment encoding for 18S rRNA . Lane 1; $h^{+N}ubc7^{+}$ (JY746); lane 2, $h^{90}ubc7^{+}$ (JY878); lanes 3 and 4, $h^{+N}ubc7^{-}$ (PY32); lane 5 , $h^{90}ubc7^{-}$ (PY45).

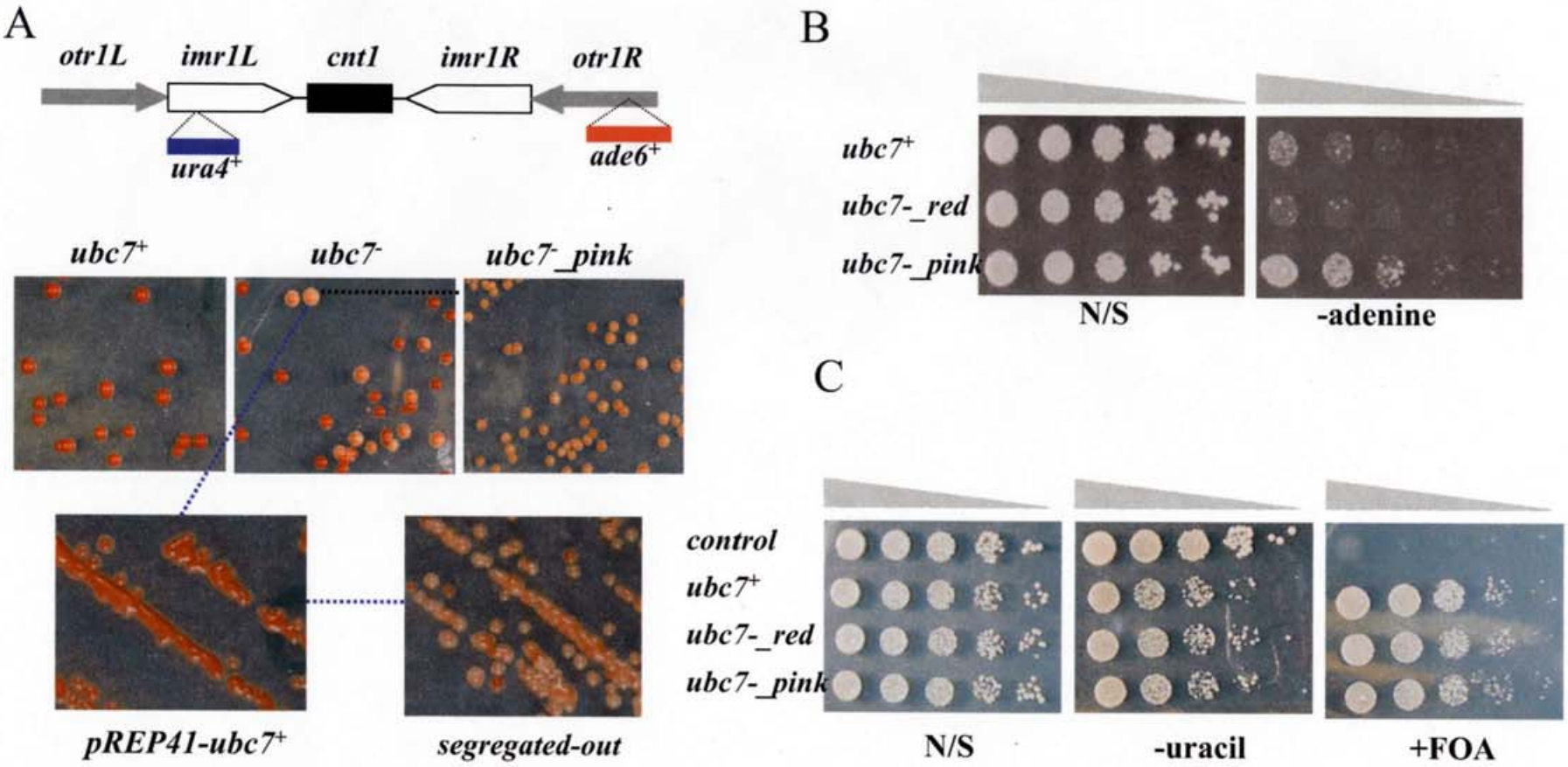

Fig. 12. The effect of the Ubc7-defect on centromeric silencing. (A) The heterogeneity of the color of colonies caused by inactivation of Ubc7. The insertion of marker genes of the tester strain FY1193 is also shown. (B) Tenfold serial dilutions of freshly grown cells were spotted on either non-selective (N/S) or adenine-free plate. (C) The *ubc7* mutation did not affect silencing of the *ura4*$^+$ gene inserted in the *imr1L* region. Cells were grown, and spotted onto non-selective (N/S), uracil-free or counterselective FOA plate and grown for five days before being photographed. *S.pombe* strains shown are as follows; *ubc7*$^+$, FY1193; *ubc7*$^-$, PYK52; *ubc7*$^-$*_pink* , pink colony from PYK52; *ubc7*$^-$*_red*, red colony from PYK52; *pREP41-ubc7*$^+$, *ubc7*$^-$*_pink* carrying *pREP41-ubc7*$^+$; *segregated-out*, *ubc7*$^-$*_pink* carrying no cDNA; *control*, PYK44 (*ura4*$^+$ random int.).

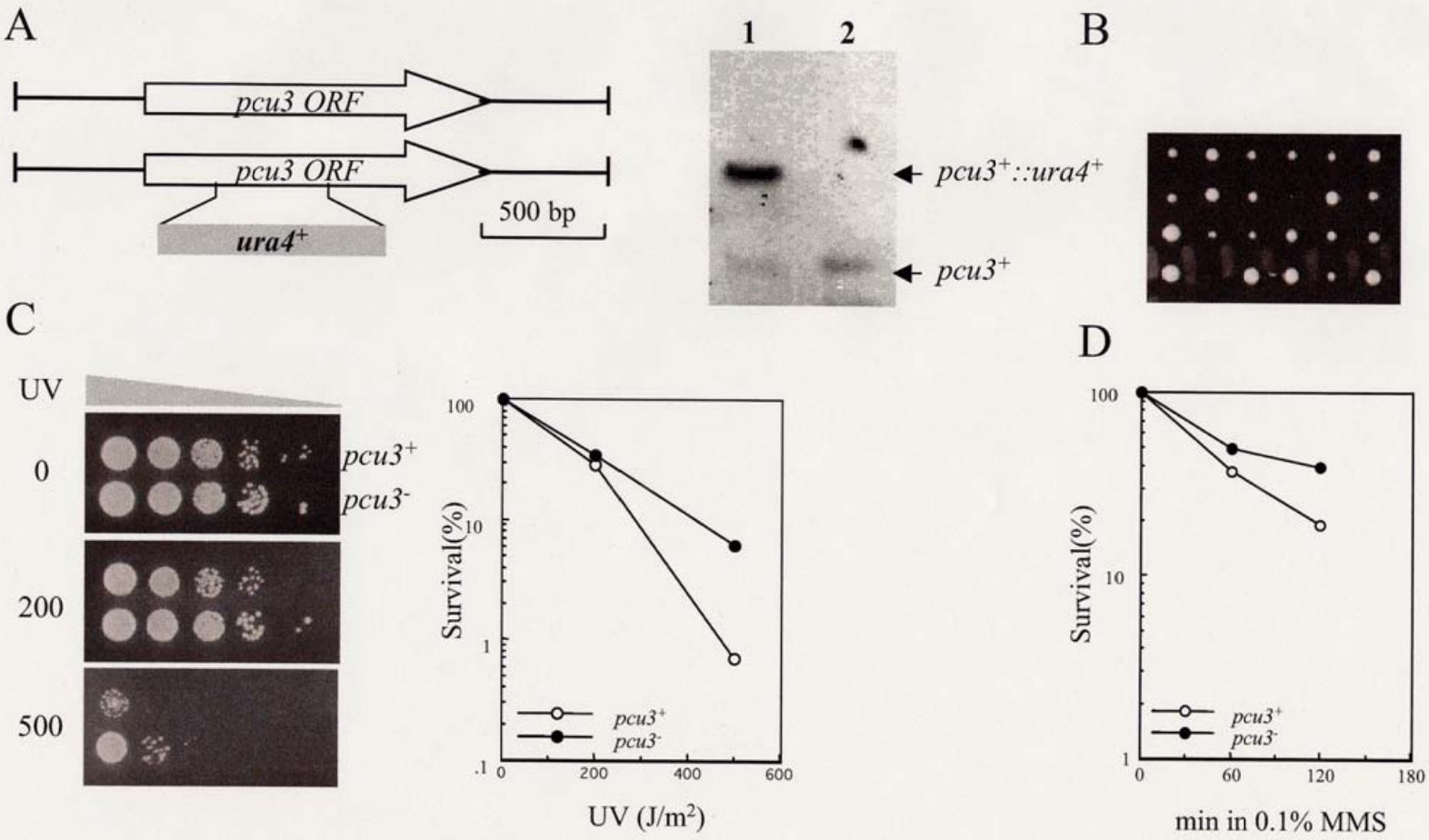

Fig. 13. Pcu3 is not essential for cell growth and its mutation results in the hyper-resistance to DNA damage. (A) One copy of the *pcu3*$^+$ gene was disrupted in diploid strain JY765. The correct knock-out was confirmed by Southernt analysis. (B) Tetrad dissection of the resulting heterozygous diploid for *pcu3*. (C) UV sensitivity assay. Cells were grown to mid-log phase, spotted onto YES medium, and followed by UV irradiation at indicated doses (left panel). The right panel indicates a quantitative result. (C) MMS sensitivity was also examined as shown in Fig. 10B. The *pcu3*$^-$ cells (PY52;closed circles) were hyper-resistant to both UV and MMS compared to the *pcu3*$^+$ (Z436;open circles) cells.